Mathematical
Inequalities
& Applications
Volume 20, Number 2 (2017), 301–348 doi:10.7153/mia-20-22

A COMPLETE 3–DIMENSIONAL BLASCHKE–SANTALÓ DIAGRAM

RENÉ BRANDENBERG AND BERNARDO GONZÁLEZ MERINO

(*Communicated by H. Martini*)

Abstract. We present a complete 3-dimensional Blaschke-Santaló diagram for planar convex bodies with respect to the four classical magnitudes: inradius, circumradius, diameter, and (minimal) width in Euclidean spaces.

1. Introduction

The focus of this paper is on the standard radii measured for the family $\mathscr{K}^n$ of convex bodies (compact and convex sets) $K \subset \mathbb{R}^n$. The *diameter* $D(K)$ of K is the largest distance between two points of K. The *width* $w(K)$ is the minimal *breadth*, i. e. the smallest distance between any two different parallel supporting hyperplanes of K. The *inradius* $r(K)$ is the radius of a largest ball contained in K, and the *circumradius* $R(K)$ is the radius of the (unique) smallest ball containing K.

A natural and very intuitive question is the following: if $K \in \mathscr{K}^n$ is given and we have fixed values for some of the previous radii (say e. g. r, D and R), what is the range of possible values of w depending on r, D and R? A comprehensive solution of this task in $\mathscr{K}^2$ is presented in the following in form of a Blaschke-Santaló diagram (sometimes also called shape diagram).

Let us start with some historical and more general review: in [1] Blaschke proposed the study of possible values for the volume $V(K)$, surface area $S(K)$, and integral mean curvature $M(K)$ for any $K \in \mathscr{K}^3$. For doing so, he considered the mapping

$$h : \mathscr{K}^3 \to [0,1]^2, \text{ with } h(K) := \left(\frac{4\pi S(K)}{M(K)^2}, \frac{48\pi^2 V(K)}{M(K)^3}\right).$$

The image $h(\mathscr{K}^3)$ is known as *Blaschke diagram*. Blaschke realized that the isoperimetric inequality and the geometric inequalities of Minkowski were not sufficient for a complete description of $h(\mathscr{K}^3)$. A *complete system of inequalities* needed additional geometric inequalities relating V, S and M, still a famous open problem in convex geometry [14, 18].

Mathematics subject classification (2010): Primary 52A10, 52A40; Secondary 52A20.
Keywords and phrases: Inradius, circumradius, geometric inequalities, Blaschke diagram, Blaschke-Santaló diagram, shape diagrams.
The second author was partially supported by MINECO (Ministerio de Economía y Competitividad) and FEDER (Fondo Europeo de Desarrollo Regional) project MTM2012-34037, and La Fundación Séneca Región de Murcia, under the programme *Becas-contrato predoctorales de formación del personal investigador*, 2008.

Reviving the idea of Blaschke, Santaló proposed in [19] the study of such diagrams for all triples of the magnitudes r, w, D, R, p (perimeter) and A (area) (initially for planar sets). Once a triple is fixed, say (r,D,R), the corresponding function

$$g : \mathscr{K}^2 \to [0,1]^2, \text{ with } g(K) := \left(\frac{r(K)}{R(K)}, \frac{D(K)}{2R(K)}\right)$$

is considered, and its image $g(\mathscr{K}^2)$ is called a *Blaschke-Santaló diagram*. Full descriptions of such diagrams for the triples (A,p,w), (A,p,r), (A,p,R), (A,w,D), (p,w,D), and (r,D,R) are already derived in [19].

The first important ingredients to start the full description of the diagram for (r,D,R) in [19] are the chain of well known (and easy to prove) inequalities

$$2r(K) \leqslant w(K) \leqslant D(K) \leqslant 2R(K) \tag{1}$$

as well as the inequality of Jung [16]

$$R(K) \leqslant \sqrt{\frac{n}{2(n+1)}} D(K) \tag{2}$$

which are true for all $K \in \mathscr{K}^n$.

The validity of the inequalities

$$w(K) \leqslant r(K) + R(K) \leqslant D(K) \tag{3}$$

was shown in [19] (there only for $n = 2$, but easy to see to be true in general dimensions, see e. g. [4]). Equality in (3) holds true simultaneously, iff K is of constant width. See [6] for more details and extensions of (3).

A final inequality derived in [19] holds true (in the given form) for $K \in \mathscr{K}^2$ only:

$$2R(K)\left(2R(K) + \sqrt{4R(K)^2 - D(K)^2}\right) r(K) \geqslant D(K)^2 \sqrt{4R(K)^2 - D(K)^2},$$

with equality, if K is an isosceles triangle.

This inequality, together with Jung's inequality (2) and the relevant parts of (1) and (3) forms a complete system of inequalities for (r,D,R).

Moreover, Santaló observed that previously known inequalities did not form complete systems of inequalities in any case of changing one of (r,D,R) to the width w.

Dekster in [9] and Hernández Cifre and Segura Gomis in [12, 15] found the missing inequalities:

$$\begin{aligned} (4R(K)^2 - D(K)^2)D(K)^4 &\leqslant 4w(K)^2R(K)^4, \\ (4r(K) - w(K))(w(K) - 2r(K))R(K) &\leqslant 2r(K)^3, \\ D(K)^4(w(K) - 2r(K))^2(4r(K) - w(K)) &\leqslant 4r(K)^4 w(K), \qquad \text{and} \\ \sqrt{3}\,(w(K) - r(K)) &\leqslant D(K). \end{aligned}$$

Hernández Cifre and Segura Gomis showed that the new inequalities together with (1) to (3) (restricted to those involving the appropriate radii) form complete systems of inequalities for the triples (w,D,R), (r,w,R), and (r,w,D). In [13] Hernández Cifre computed complete systems of inequalities for the triples (A,D,R) and (p,D,R) and Böröczky Jr., Hernández Cifre, and Salinas gave complete diagrams for the triples (A,r,R) and (p,r,R) in [3].

There are still 7 out of the 20 possible triples involving also A and p where a full description of the diagram is still missing. However, all 4 Blaschke-Santaló diagrams of $\mathcal{K}^2$ involving only the classical radii r,w,D, and R have been completed, which means not only knowing a (minimal) complete system of inequalities describing them, but also the extreme sets inducing the boundaries of the diagrams (which is possibly more important).

Recently, Blaschke-Santaló diagrams have been used in pattern recognition and image analysis (see [7, 8, 17]), as they help in the prediction of the size and shape of 3-dimensional sets from their 2-dimensional projections. In [7, 17] for example, the diagrams (in this context mostly called shape-diagrams) have been combined with probabilistic methods, e. g. maximum likelihood estimation in [17].

Once there are complete systems of inequalities for some of the possible triples of magnitudes amongst A,p,r,w,D,R, it is a natural step to consider complete systems of inequalities for even more than three of those magnitudes, e. g. to obtain stronger inequalities or for an even more accurate classification of convex sets in the mentioned application in image analysis. In [23] the quadruple (A,p,w,D) has been considered, without deriving a complete description (which is not so surprising, as even for the triple (A,p,D) a complete description is still missing). We consider the case (r,w,D,R), which is the unique diagram involving four of the above magnitudes, s. t. complete descriptions of the diagrams are known for all subsets of three of these magnitudes. To the best of our knowledge, besides [23] and the preliminary work of this paper in [4], this is the only paper considering more than three of these magnitudes.

The study shows the necessity of *new inequalities* relating all four radii at once. This is done by describing the diagram's skeleton, i. e. its boundary structure consisting of 0-,1-, and 2-dimensional differential manifolds (see below for a proper definition).

We now introduce some notation related to convex geometry. If $l \in \mathbb{N}$, we abbreviate $[l] := \{1,\dots,l\}$. For a general set $C \subset \mathbb{R}^n$, we write $\mathrm{aff}(C)$ and $\mathrm{conv}(C)$ for the *affine hull* and the *convex hull* of C, respectively. For any $x,y \in \mathbb{R}^n$ we denote by $[x,y]$ the *segment* $\mathrm{conv}\{x,y\}$ whose endpoints are x and y. If $K \in \mathcal{K}^n$ we write $\mathrm{ext}(K)$ for the set of *extreme points* of K and any $x \in \mathrm{ext}(K)$ is said to be *exposed*, if there exists a hyperplane H supporting K, s. t. $K \cap H = \{x\}$.

The Euclidean unit ball and unit sphere are denoted by $\mathbb{B},\mathbb{S} \subset \mathbb{R}^n$, respectively, and the closed (open) *semisphere* $\{x \in \mathbb{S} : u^T x \geqslant 0\}$ (respectively $\{x \in \mathbb{S} : u^T x > 0\}$) with $u \in \mathbb{R}^n \setminus \{0\}$, by $\mathbb{S}_u^{\geqslant}$ ($\mathbb{S}_u^{>}$). By $\mathrm{dist(A,B)}$ we denote the usual Euclidean distance between two closed sets $A,B \subset \mathbb{R}^n$, and write $\mathrm{dist(a,B)}$ or $\mathrm{dist(A,b)}$ if one of the sets is a singleton.

For a pair of bodies $K,L \in \mathcal{K}^n$, the *Minkowski sum* of K and L is defined as $K+L := \{x_1+x_2 : x_1 \in K, x_2 \in L\}$. The λ *dilatation* of K with $\lambda \in \mathbb{R}$ is $\lambda K := \{\lambda x : x \in K\}$. We abbreviate $K-L := K+(-L)$ and $K+x := K+\{x\}$ for $x \in \mathbb{R}^n$. A body

K is 0-*symmetric* if $K = -K$ and *centrally symmetric* if there exists $c \in \mathbb{R}^n$, s. t. $K - c$ is 0-symmetric.

For any body $K \in \mathcal{K}^n$, a *completion* of K is defined as a set K^* satisfying $K \subset K^*$ and $D(K) = D(K^*) = w(K^*)$. Moreover, K^* is called a *Scott-completion* of K if, in addition, $R(K) = R(K^*)$ (it was shown in [21] that in Euclidean space such a completion always exists).

The next three propositions will be useful below. The first collects results taken from [10]:

PROPOSITION 1.1. *For any* $K \in \mathcal{K}^n$

a) *every pair of points* $p, q \in K$ s. t. $\|p - q\| = D(K)$ *is a pair of exposed (and therefore extreme) points in* K.

b) *every pair* L_1, L_2 *of parallel supporting hyperplanes of* K *at distance* $w(K)$ *supports a segment with endpoints in* $K \cap L_1$ *and* $K \cap L_2$ *perpendicular to both hyperplanes. Moreover, if* $K \in \mathcal{K}^n$ *is a polyhedron, then* $\dim(K \cap L_1) + \dim(K \cap L_2) \geqslant n - 1$ *(which in case of* $n = 2$ *means that at least one of the intersections* $K \cap L_i$, $i = 1, 2$, *contains a segment).*

The first part of the following proposition about the Euclidean circumradius was shown already in [2]. For the part about the inradius we refer to the general optimality conditions for containment under homothetics given in [5].

PROPOSITION 1.2. *Let* $K \in \mathcal{K}^n$ *and* $c \in \mathbb{R}^n$ *be* s. t. $c + \rho\mathbb{B} \subseteq K \subset \mathbb{B}$. *Then*

a) $R(K) = 1$, *iff there exist* $k \in \{2, \dots, n+1\}$ *and* $p^1, \dots, p^k \in \mathrm{bd}(K) \cap \mathbb{S}$, s. t. $0 \in \mathrm{conv}\{p^1, \dots, p^k\}$.

b) $r(K) = \rho$, *iff there exist* $l \in \{2, \dots, n+1\}$, $q^1, \dots, q^l \in \mathrm{bd}(K - c) \cap \rho\mathbb{S}$, *and* $u^1, \dots, u^l \in \mathbb{S}$, s. t. $(u^i)^T q^i = \rho$, $i \in [l]$, $K - c \subset \bigcap_{i \in [l]} \{x \in \mathbb{R}^n : (u^i)^T x \leqslant \rho\}$, *and* $0 \in \mathrm{conv}\{u^1, \dots, u^l\}$.

The third proposition is ancient and best known as the "inscribed angle theorem":

PROPOSITION 1.3. *For any triangle* $T := \mathrm{conv}\{p^1, p^2, p^3\}$ *with* $p^1, p^2, p^3 \in \mathbb{S}$ *and 0 and* p^3 *on the same side of* $\mathrm{aff}\{p^1, p^2\}$ *let* γ *denote the angle of* T *at* p^3. *Then the angle of the triangle* $\mathrm{conv}\{p^1, p^2, 0\}$ *at 0 is* 2γ *(independently of the position of* p^3*).*

Moreover, if $p^3 \in \mathrm{int}(\mathbb{B})$ *(respectively* $p^3 \notin \mathbb{B}$*), but still on the same side of* $\mathrm{aff}\{p^1, p^2\}$ *than 0, the angle in 0 is strictly smaller (or, respectively, strictly greater) than* 2γ.

The remainder of the paper is organized as follows: in Section 2 the way we proceed for the description of the whole diagram is explained.

In Section 3 we present a collection of nine (generally) valid inequalities completely describing the diagram in Section 2. Six of these inequalities were known before but three of them are totally new, relating all four basic radii at once (in a non-redundant way).

Since all inequalities have an algebraic representation, every family of sets attaining equality in one of the inequalities above is mapped onto a compact connected subset of a 2-dimensional differential manifold within $\mathbb{R}^3$. We call them *facets* of the diagram. Moreover, the common boundaries between any two facets are called *edges* of the diagram and the bodies appearing in the intersection of three (or more) facets are called *vertices* of the diagram. The families forming the facets and edges, as well as all vertices are described in Section 4.

Section 5 is devoted to the proofs of the new inequalities presented in Section 3, while the paper concludes with some directions for future research in Section 6.

2. Main ideas for explaining the diagram

Following the idea of Blaschke and Santaló, we define

$$f : \mathcal{K}^n \to [0,1]^3, \quad f(K) = \left(\frac{r(K)}{R(K)}, \frac{w(K)}{2R(K)}, \frac{D(K)}{2R(K)} \right) \tag{4}$$

and call $f(\mathcal{K}^n)$ a *3-dimensional Blaschke-Santaló diagram*. The following is taken from [4].

LEMMA 2.1. *$f(\mathcal{K}^n) = f(\{K \in \mathcal{K}^n : \mathbb{B}$ is the circumball of $K\})$ is starshaped with respect to $f(\mathbb{B}) = (1,1,1)$.*

Proof. For $K \in \mathcal{K}^n$, $c \in \mathbb{R}^n$, $\lambda \in [0,1]$, and q being any of the four radii functionals r, w, D, R, it obviously holds $q(\lambda(K+c)) = \lambda q(K)$ and $q(\lambda K + (1-\lambda)\mathbb{B}) = \lambda q(K) + (1-\lambda)q(\mathbb{B})$. □

Lemma 2.1 means that the diagram has no "holes" and therefore it suffices to describe the sets $K \in \mathcal{K}^n$, with circumball $\mathbb{B}$, such that $f(K) \in \mathrm{bd}(f(\mathcal{K}^n))$.

LEMMA 2.2. *Let $K, K^* \in \mathcal{K}^n$ be* s. t. *K^* is a completion of K and $K_\lambda := \lambda K + (1-\lambda)K^*$, $\lambda \in [0,1]$. Then $D(K_\lambda) = D(K)$ and $w(K_\lambda) = \lambda w(K) + (1-\lambda)w(K^*)$.*

Proof. Since $K \subset K^*$ and $D(K) = D(K^*)$ it immediately follows from $K \subset K_\lambda \subset K^*$ that $D(K_\lambda) = D(K)$ for every $\lambda \in [0,1]$. Now, let $s^* \in \mathbb{S}$ be s. t. the breadth $b_{s^*}(K)$ of K in direction of s^* is $b_{s^*}(K) = w(K)$. Since K^* is of constant width and because the breadth is linear with respect to the Minkowski sum, we obtain that

$$\begin{aligned} w(K_\lambda) &= \min_{s \in \mathbb{S}} b_s(K_\lambda) = \min_{s \in \mathbb{S}} (\lambda b_s(K) + (1-\lambda) b_s(K^*)) \\ &\leqslant \lambda b_{s^*}(K) + (1-\lambda) w(K^*) = \lambda w(K) + (1-\lambda) w(K^*) \leqslant w(K_\lambda). \quad \square \end{aligned}$$

LEMMA 2.3. *For any $K \in \mathcal{K}^n$ satisfying the left inequality in (3) with equality (*i. e. *$w(K) = r(K) + R(K)$), K^* being its Scott-completion, and $K_\lambda := \lambda K + (1-\lambda)K^*$, $\lambda \in [0,1]$, it holds that $f(K_\lambda) = \lambda f(K) + (1-\lambda) f(K^*)$ and therefore $w(K_\lambda) = r(K_\lambda) + R(K_\lambda)$.*

Proof. Using Lemma 2.2 it immediately follows that $D(K_\lambda) = D(K)$, $R(K_\lambda) = R(K)$, and $w(K_\lambda) = \lambda w(K) + (1-\lambda) w(K^*)$ for all $\lambda \in [0,1]$.

In [4] it was shown that $w(K) = r(K) + R(K)$ implies that K has a unique inball being concentric with the circumball. Now, restricting again to such sets K having $\mathbb{B}$ as their circumball, we obtain that $r(K)\mathbb{B} \subset K \subset \mathbb{B}$ with $R(K) = 1$.

Observe that if $s \in \mathbb{S}$ with $-r(K)s \in \mathrm{bd}(K)$, then $s \in K$. This follows because a supporting hyperplane in $-r(K)s$ of K has to support $r(K)\mathbb{B}$ too, and therefore this hyperplane has to be $-r(K)s + \mathrm{lin}\{s\}^\perp$. Thus the breadth of K in the direction s is at most $r(K) + R(K)$, with equality iff $s \in K$.

Because of Part (b) in Proposition 1.2 there exist $u^1, \ldots, u^j \in \mathbb{S}$, s. t. $-r(K)u^i \in \mathrm{bd}(K)$, $i \in [j]$ with $0 \in \mathrm{conv}\{u^1, \ldots, u^j\}$. Together with the observation above this yields that $u^i \in K \cap \mathbb{S}$ and that the hyperplanes $-r(K)u^i + \mathrm{lin}\{u^i\}^\perp$ support K in $-r(K)u^i$, $i \in [j]$.

Now, because K^* is a Scott-completion of K it obviously holds $r(K^*)\mathbb{B} \subset K^* \subset \mathbb{B}$, $u^i \in K^*$, $i \in [j]$. Since $w(K^*) = r(K^*) + R(K^*)$ it also holds that the hyperplanes $-r(K^*)u^i + \mathrm{lin}\{u^i\}^\perp$ support K^* and its inball in $-r(K^*)u^i$, $i \in [j]$. Altogether we obtain that $-r(K)u^i + \mathrm{lin}\{u^i\}^\perp$ and $-r(K^*)u^i + \mathrm{lin}\{u^i\}^\perp$ support K and K^* in the points $-r(K)u^i$ and $-r(K^*)u^i$, respectively. Hence the hyperplanes $-(\lambda r(K) + (1-\lambda) r(K^*))u^i + \mathrm{lin}\{u^i\}^\perp$ support $\lambda K + (1-\lambda)K^*$ in the points $-(\lambda r(K) + (1-\lambda) r(K^*))u^i$, $i \in [j]$. Using again Part (b) in Proposition 1.2, it follows $r(\lambda K + (1-\lambda)K^*) = \lambda r(K) + (1-\lambda) r(K^*)$ and from this the lemma follows. □

As mentioned in Section 1 the inequalities

$$\begin{aligned} &D(K) \leqslant 2R(K), \quad D(K) \geqslant r(K) + R(K), \quad D(K) \geqslant \sqrt{3}R(K), \quad \text{and} \\ &2R(K)\left(2R(K) + \sqrt{4R(K)^2 - D(K)^2}\right) r(K) \geqslant D(K)^2 \sqrt{4R(K)^2 - D(K)^2}, \end{aligned} \tag{5}$$

give a full description of

$$g : \mathcal{K}^2 \to [0,1]^2, \text{ with } g(K) := \left(\frac{r(K)}{R(K)}, \frac{D(K)}{2R(K)}\right)$$

(see Figure 1).

Since $g(\mathcal{K}^2)$ is just the projection of $f(\mathcal{K}^2)$ onto the first and last coordinate, we may consider any valid pair of values $(r, D/2) \in g(\mathcal{K}^2)$ and solve

$$\begin{array}{rl} \max_{K \in \mathcal{K}^2} & w(K) \\ & r(K) = r \\ & D(K) = D \\ & R(K) = 1 \end{array} \qquad \text{as well as} \qquad \begin{array}{rl} \min_{K \in \mathcal{K}^2} & w(K) \\ & r(K) = r \\ & D(K) = D \\ & R(K) = 1\,. \end{array}$$

Calling the solution of the maximization problem $w^*(r,D)$ for any given pair $(r, D/2)$ and the solution of the minimization problem $w_*(r,D)$, the families

$$\{w^*(r,D) : (r,D/2) \in g(\mathcal{K}^2)\} \quad \text{and} \quad \{w_*(r,D) : (r,D/2) \in g(\mathcal{K}^2)\}$$

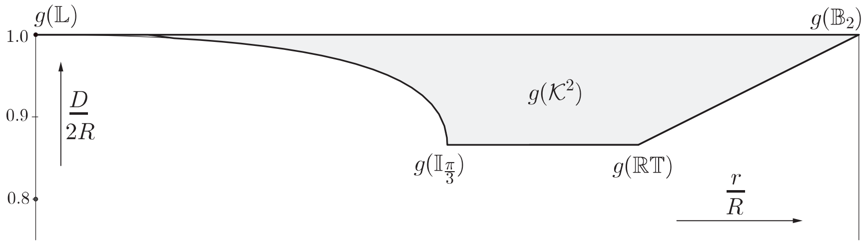

Figure 1: *The diagram $g(\mathscr{K}^2)$ with x-axis ${}^{r}/_{R}$ and y-axis ${}^{D}/_{2R}$. The boundaries are given via the inequalities collected in (5). The vertices are the Euclidean ball $\mathbb{B}$, the line segment $\mathbb{L}$, the equilateral triangle $\mathbb{I}_{\pi/3}$ and the Reuleaux triangle $\mathbb{RT}$ (see Subsection 4.1 for their explanation).*

describe the upper and lower boundary of $f(\mathscr{K}^2)$, respectively. To complete the full diagram it now suffices to check the following: which of the inequalities in (5) still describe facets of $f(\mathscr{K}^2)$ and which describe only edges. The former is the case if there exists a pair $(r,D/2) \in \mathrm{bd}(g(\mathscr{K}^2))$, s. t. the corresponding inequality is fulfilled with equality and $w^*(r,D) \neq w_*(r,D)$. The latter is the case if $w^*(r,D) = w_*(r,D)$ for all $(r,D/2) \in g(\mathscr{K}^2)$ fulfilling the inequality with equality.

3. Main inequalities

In this section we describe nine valid inequalities for $f(\mathscr{K}^2)$. Three of them are of the form $w \leqslant w^*(r,D)$, thus describing the upper boundary of the diagram; we call them (ub_j), $j = 1,2,3$. Analogously, we write (lb_j), $j = 1,2,3$ for the three inequalities $w \geqslant w_*(r,D)$ (giving the lower boundary) and finally (ib_j), $j = 1,2,3$ for the inequalities which are independent of w.

We start with those inequalities which are a-priori known:

PROPOSITION 3.1. *Let $K \in \mathscr{K}^2$. Then*

$$2r(K) \leqslant w(K) \qquad (lb_1)$$

$$D(K) \leqslant 2R(K) \qquad (ib_1)$$

$$w(K) \leqslant R(K) + r(K) \qquad (ub_1)$$

$$R(K) + r(K) \leqslant D(K) \qquad (ib_2)$$

$$\sqrt{3}R(K) \leqslant D(K) \qquad (ib_3)$$

$$(4R(K)^2 - D(K)^2)D(K)^4 \leqslant 4w(K)^2R(K)^4 \qquad (lb_2)$$

The remaining three inequalities for a complete description of $f(\mathscr{K}^2)$ are new. Clearly, each of them involves all four radii r, w, D, and R simultaneously as otherwise it would have been necessary for the description of the corresponding 2-dimensional Blaschke-Santaló diagram.

THEOREM 3.2. *Let $K \in \mathcal{K}^2$. Then*

$$w(K) \geqslant 2D(K)\sqrt{1-\left(\frac{D(K)}{2R(K)}\right)^2} \cos\left[\arccos\left(\frac{D(K)}{2(D(K)-r(K))}\right)+\arccos\left(\frac{D(K)}{2R(K)}\right)-\arcsin\left(\frac{r(K)}{D(K)-r(K)}\right)\right] \tag{lb_3}$$

REMARK 3.3. An algebraic representation of (lb_3) can easily be calculated using a computer algebra tool and looks like the following:

$$w(K) \geqslant 2D(K)\sqrt{1-\left(\frac{D(K)}{2R(K)}\right)^2}\left[\sqrt{1-\frac{r(K)^2}{(D(K)-r(K))^2}}\left(\frac{D(K)^2}{4R(K)(D(K)-r(K))}\right.\right.$$
$$\left.-\sqrt{\left(1-\frac{D(K)^2}{4(D(K)-r(K))^2}\right)\left(1-\frac{D(K)^2}{4R(K)^2}\right)}\right)+\frac{r(K)}{D(K)-r(K)}$$
$$\left.\left(\frac{D(K)}{2R(K)}\sqrt{1-\frac{D(K)^2}{4(D(K)-r(K))^2}}-\frac{D(K)}{2(D(K)-r(K))}\sqrt{1-\frac{D(K)^2}{4R(K)^2}}\right)\right]$$

THEOREM 3.4. *Let $K \in \mathcal{K}^2$. Then*

$$w(K) \leqslant r(K)\left(1+\frac{2\sqrt{2}R(K)}{D(K)}\sqrt{1+\sqrt{1-\left(\frac{D(K)}{2R(K)}\right)^2}}\right) \tag{ub_2}$$

THEOREM 3.5. *Let $K \in \mathcal{K}^2$. Then*

$$w(K) \leqslant 2r(K)\left(1+\frac{2r(K)R(K)}{D(K)^2}\left(1+\sqrt{1-\left(\frac{D(K)}{2R(K)}\right)^2}\right)\right) \tag{ub_3}$$

REMARK 3.6. One may recognize that

$$1+\frac{(2\sqrt{2}R(K))}{D(K)}\sqrt{1+\sqrt{1-\left(\frac{D(K)}{2R(K)}\right)^2}} \leqslant 3,$$

which shows that (ub_2) is a direct strengthening of the 2-dimensional version of Steinhagen's inequality (cf. [22]). However, this is not the case for (ub_3) (even so the two sets $\mathbb{L}$ and $\mathbb{I}_{\pi/3}$ fulfilling Steinhagen's inequality with equality fulfill (ub_3) with equality, too) as, e. g. evaluating (ub_3) at $\mathbb{RT}$ gives

$$\frac{w(\mathbb{RT})}{r(\mathbb{RT})} \leqslant 3 < 2\left(1+\frac{2r(\mathbb{RT})R(\mathbb{RT})}{D(\mathbb{RT})^2}\left(1+\sqrt{1-\left(\frac{D(\mathbb{RT})}{2R(\mathbb{RT})}\right)^2}\right)\right).$$

It is also quite easy to see that for an equivalent of our diagram for higher dimensional sets Steinhagen's inequality induces a facet.

4. The skeleton of the 3-dimensional diagram

This section is devoted to the description of families of bodies filling the faces of $\mathrm{bd}(f(\mathcal{K}^2))$.

We start in Subsection 4.1 describing the sets fulfilling three or more inequalities with equality, the vertices of $\mathrm{bd}(f(\mathcal{K}^2))$. In Subsection 4.2 we discuss the families of sets fulfilling two inequalities with equality, the edges of $\mathrm{bd}(f(\mathcal{K}^2))$. Finally, in Subsection 4.3 families of sets filling the different facets are explained. For the description of these sets we always assume that $\mathbb{B}$ is the circumball, but for a better understanding of the geometric inequalities we will keep the value $R(K)$ in each description.

In case there does not exist a unique set, which is mapped to a boundary point of the diagram, we will usually describe in some way the range of sets mapped to that point, e. g. by giving maximal and minimal sets (with respect to set inclusion) if appropriate. However, as this is not our main topic, we neither claim completeness nor present detailed proofs.

4.1. Vertices of the diagram

The vertices, including their radii, and for each the inequalities which are fulfilled with equality are listed in the following:

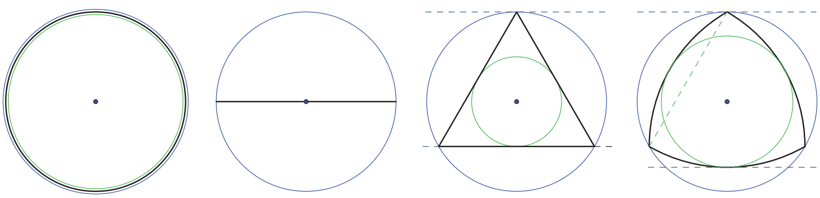

Figure 2: *From left to right: the Euclidean ball $\mathbb{B}$, the line $\mathbb{L}$, the equilateral triangle $\mathbb{I}_{\pi/3}$, and the Reuleaux triangle $\mathbb{RT}$. Here and in all the forthcoming figures, the inballs are drawn in green, the circumballs in blue, the diameters in dashed green, and the widths in dashed blue.*

$\mathbb{B}$ Obviously, the *Euclidean ball* $\mathbb{B}$ is the unique set mapped to $f(\mathbb{B}) = (1,1,1)$ in the diagram. It is extreme for the inequalities (lb_1), (ib_1), (ub_1), and (ib_2).

$\mathbb{L}$ The radii of the *line segment* $\mathbb{L}$ are easy to see, too: $f(\mathbb{L}) = (0,0,1)$ and also it is the only set mapped to these coordinates. The inequalities it fulfills with equality are (lb_1), (lb_2), (ib_1), and (ub_3). It also fulfills (ub_2) with equality, but this is an artefact which will be explained in Remark 4.1.

$\mathbb{I}_{\pi/3}$ The coordinates $f(\mathbb{I}_{\pi/3}) = \left(1/2, 3/4, \sqrt{3}/2\right)$ of the *equilateral triangle* $\mathbb{I}_{\pi/3}$ are well known. It is the unique set with these coordinates and extreme for the inequalities (ub_1), (ub_2), (ub_3), (lb_2), and (ib_3).

$\mathbb{RT}$ The *Reuleaux triangle* $\mathbb{RT}$ is the intersection of three Euclidean balls of radius $\sqrt{3}$ centered at the vertices of $\mathbb{I}_{\pi/3}$. On the one hand it has the same diameter and circumradius as $\mathbb{I}_{\pi/3}$. On the other hand it is of constant width, thus (lb_1) and (ib_2) imply $w(\mathbb{RT}) = r(\mathbb{RT}) + R(\mathbb{RT}) = D(\mathbb{RT})$. Hence $f(\mathbb{RT}) = (\sqrt{3}-1, \sqrt{3}/2, \sqrt{3}/2)$ and $\mathbb{RT}$ is the unique set mapped to this point of the diagram. It is extreme for the inequalities (ub_1), (ib_2) and (ib_3).

$\mathbb{I}_{\pi/2}$ The *(isosceles) right-angled triangle* $\mathbb{I}_{\pi/2}$ (for brevity we will sometimes omit the term "isosceles") has diameter $D(\mathbb{I}_{\pi/2}) = 2R(\mathbb{I}_{\pi/2})$ and its width coincides with its height above the diameter edge, thus $w(\mathbb{I}_{\pi/2}) = R(\mathbb{I}_{\pi/2})$. Using the semiperimeter formula for triangles, we obtain that the inradius is

$$r(\mathbb{I}_{\pi/2}) = \frac{D(\mathbb{I}_{\pi/2})w(\mathbb{I}_{\pi/2})}{D(\mathbb{I}_{\pi/2}) + 2\sqrt{2}R(\mathbb{I}_{\pi/2})} = \frac{R(\mathbb{I}_{\pi/2})}{1+\sqrt{2}} = (\sqrt{2}-1)R(\mathbb{I}_{\pi/2}).$$

Thus $f(\mathbb{I}_{\pi/2}) = (\sqrt{2}-1, 1/2, 1)$ and there is no other K mapped to this coordinates (as one may easily see in following the construction of a set mapped to these coordinates). $\mathbb{I}_{\pi/2}$ is extreme for the inequalities (ub_2), (ub_3) and (ib_1).

$\mathbb{SB}$ The *(right-angled concentric) sailing boat* $\mathbb{SB}$ is the intersection of $\mathbb{B}$ and a homothet of $\mathbb{I}_{\pi/2}$ with incenter at 0 and a vertex v located where the two edges of equal length intersect on $\mathbb{S}$ (see Figure 3(a)). Hence the in- and circumball of $\mathbb{SB}$ are concentric and one can easily see from the construction, that $1/2\, D(\mathbb{SB}) = \sqrt{2}r(\mathbb{SB}) = R(\mathbb{SB})$. Its width is attained in the orthogonal directions to any three of the edges of $\mathbb{I}_{\pi/2}$. In particular by measuring between v and its opposite edge, we obtain that

$$w(\mathbb{SB}) = r(\mathbb{SB}) + R(\mathbb{SB}) = (1/\sqrt{2}+1)R(\mathbb{SB})$$

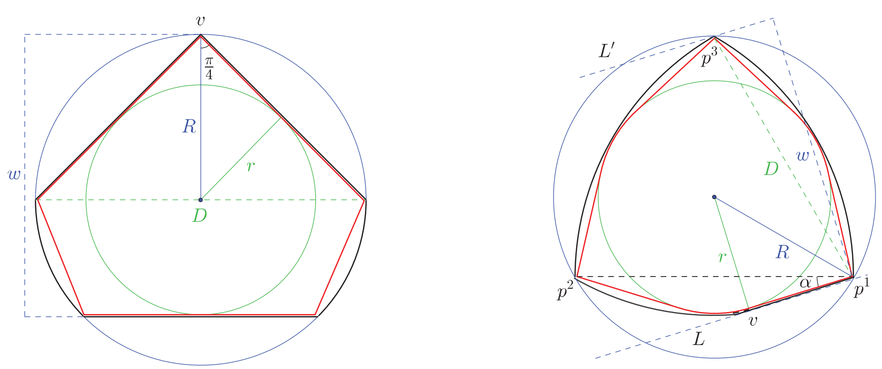

(a) *The sailing boat* $\mathbb{SB}$ *in black and the pentagon* $\mathbb{CP}$ *(sharing the vertices with* $\mathbb{SB}$*) in red.*

(b) *The sliced Reuleaux triangle* $\mathbb{SR}$ *in black and* $\mathbb{SR}_{\min}$ *(the minimal set sharing all radii with* $\mathbb{SR}$*) in red.*

Figure 3: *Sailing boats and sliced Reuleaux triangles.*

and therefore $f(\mathbb{SB}) = (1/\sqrt{2}, 1/2(1/\sqrt{2}+1), 1)$. The sailing boat fulfills inequalities (ub_1), (ub_2) and (ib_1) with equality. Finally, denoting the (circumspherical) pentagon formed from the five vertices of $\mathbb{SB}$ by $\mathbb{CP}$, we obtain that $f(K) = f(\mathbb{SB})$ for any $K \in \mathcal{K}^2$, iff $\mathbb{CP} \subset K \subset \mathbb{SB}$.

$\mathbb{SR}$ The *sliced Reuleaux triangle* $\mathbb{SR}$ is the intersection of a Reuleaux triangle $\mathbb{RT}$ and a halfspace H which supports a vertex of $\mathbb{RT}$, say p^1, and the inball of $\mathbb{RT}$ in a point v (see Figure 3(b)). By construction it keeps the same diameter, in- and circumradius as $\mathbb{RT}$. The width of $\mathbb{SR}$ is attained between the parallel lines $L = \mathrm{bd}(H)$, and L' supporting $\mathbb{SR}$ in the vertex p^2 furthest from v.

Defining α to be the angle between L and the line segment $[p^2, p^3]$, where p^3 is the remaining vertex of $\mathbb{I}_{\pi/3}$, one easily computes

$$r(\mathbb{SR}) = R(\mathbb{SR}) \sin(\pi/6 + \alpha) \quad \text{and} \quad w(\mathbb{SR}) = D(\mathbb{SR}) \cos(\pi/6 - \alpha).$$

Hence $\alpha = \arcsin(r(\mathbb{SR})/R(\mathbb{SR})) - \pi/6$ and thus

$$w(\mathbb{SR}) = D(\mathbb{SR}) \cos(\pi/3 - \arcsin(r(\mathbb{SR})/R(\mathbb{SR}))).$$

We obtain $f(\mathbb{SR}) = \left(\sqrt{3}-1, \sqrt{3}/2 \cos(\pi/3 - \arcsin(\sqrt{3}-1)), \sqrt{3}/2\right)$ and extremality for the inequalities (lb_3), (ib_2) and (ib_3).

Denoting by $\mathbb{SR}_{\min}$ the convex hull of the vertices and the inball of $\mathbb{RT}$, one may easily verify that $f(K) = f(\mathbb{SR})$ for any $K \in \mathcal{K}^2$, iff $\mathbb{SR}_{\min} \subset K \subset \mathbb{SR}$.

$\mathbb{FR}$ Let $\mathbb{FR}$ be the *flattened Reuleaux triangle*, obtained by replacing two of the three edges of $\mathbb{I}_{\pi/3}$ by the corresponding arcs of $\mathbb{RT}$. It has the same circumradius, diameter and width than $\mathbb{I}_{\pi/3}$ and defining a to be the distance from the center of the inball to each vertex incident with the linear edge, it follows $a^2 = r(\mathbb{FR})^2 + 1/4 D(\mathbb{FR})^2$ and $D(\mathbb{FR}) = a + r(\mathbb{FR})$ (see Figure 4(a)). Hence $4(D(\mathbb{FR}) - r(\mathbb{FR}))^2 = 4r(\mathbb{FR})^2 + D(\mathbb{FR})^2$ and, after dividing by $D(\mathbb{FR})$, we obtain that $3D(\mathbb{FR}) = 8r(\mathbb{FR})$. Thus $f(\mathbb{FR}) = (\sqrt{27}/8, 3/4, \sqrt{3}/2)$ and hence $\mathbb{FR}$ fulfills inequalities (lb_2), (lb_3) and (ib_3) with equality.

Denoting the convex hull of $\mathbb{I}_{\pi/3}$ and the inball of $\mathbb{FR}$ by $\mathbb{FR}_{\min}$, it holds $f(K) = f(\mathbb{FR})$, iff $\mathbb{FR}_{\min} \subset K \subset \mathbb{FR}$ (see Figure 4(a)).

$\mathbb{BT}$ Let $p^1, p^2, p^3, p^4 \in \mathbb{S}$, s.t. $\mathrm{conv}\{p^1, p^2, p^3, p^4\}$ is a trapezoid with $[p^1, p^2]$ being the longer and $[p^3, p^4]$ the shorter parallel line, and s.t. $\mathrm{conv}\{p^1, p^2, p^3\}$ as well as $\mathrm{conv}\{p^1, p^2, p^4\}$ are isosceles triangles (the first with $[p^1, p^2]$, $[p^1, p^3]$ the edges of equal length, the second with $[p^1, p^2]$, $[p^2, p^4]$), s.t. in both cases the angle between the two equal edges is $\arcsin(3/4)$ (see Figure 4(b)). We write $\mathrm{I}_{\arcsin(3/4)}$ for such an isosceles triangle (cf. Subsection 4.2). Substituting the edges $[p^1, p^4]$ and $[p^2, p^3]$ by two circular arcs of radius $\|p^1 - p^2\| = D(\mathrm{I}_{\arcsin(3/4)})$ and centers p^1 and p^2, respectively, we obtain the *bent trapezoid* $\mathbb{BT}$.

By construction $\mathbb{BT}$ and $\mathrm{I}_{\arcsin(3/4)}$ have the same width w, diameter D, and circumradius $R = 1$. We prove that the inball of $\mathbb{BT}$ is tangent to the two parallels

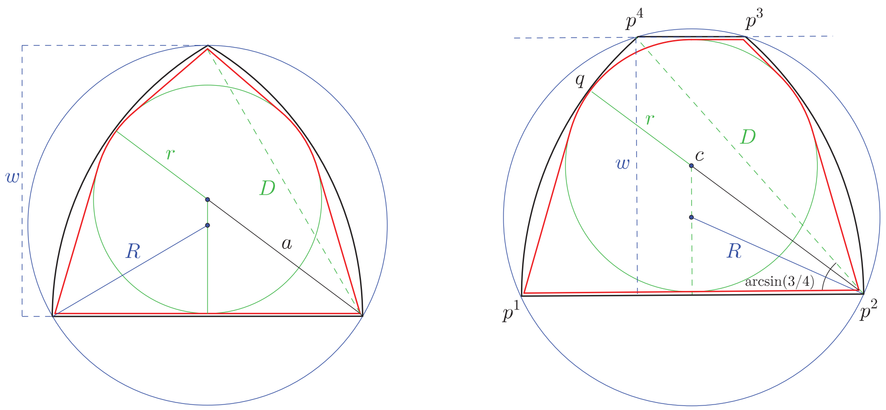

(a) *In black* $\mathbb{FR}$*, in red* $\mathbb{FR}_{\min}$.

(b) *In black* $\mathbb{BT}$*, in red* $\mathbb{BT}_{\min}$.

Figure 4: *The flattened Reuleaux triangle and the bent trapezoid.*

and the two arcs: Let B be a ball of radius $r = {}^1\!/_2 w$ and center $c = {}^1\!/_4(p^1 + p^2 + p^3 + p^4)$, and denote the intersection point of the line through p^2 and c with the arc between p^1 and p^4 by q. We show that $\|c - q\| = r$ which then implies $r(\mathbb{BT}) = r$:

$$\text{(i)}\ \ \|c-q\| = D - \left\|c-p^2\right\|, \quad \text{(ii)}\ \ r^2 + {}^1\!/_4 D^2 = \left\|c-p^2\right\|^2, \quad \text{(iii)}\ \ w = {}^3\!/_4 D.$$

From (iii) we obtain that $D = {}^8\!/_3 r$, and using (i) combined with (ii) gives

$$\|c-q\| = D - \sqrt{r^2 + {}^1\!/_4 D^2} = {}^8\!/_3 r - \sqrt{r^2 + {}^{16}\!/_9 r^2} = r,$$

as we wanted to show. Thus $r(\mathbb{BT}) = r = {}^1\!/_2 w$.

For computing D, we use the fact that the line from p^2 through 0 is the bisecting line of the angle $\arcsin({}^3\!/_4)$ between $[p^1, p^2]$ and $[p^2, p^4]$ at p^2, which means

$$\frac{D}{2R} = \frac{D(\mathrm{I}_{\arcsin({}^3/_4)})}{2R(\mathrm{I}_{\arcsin({}^3/_4)})} = \cos\left(\frac{1}{2}\arcsin\left(\frac{3}{4}\right)\right).$$

This implies

$$D = 2\cos\left({}^1\!/_2 \arcsin\left({}^3\!/_4\right)\right) R = \sqrt{2 + {}^{\sqrt{7}}\!/_2}\, R,$$

and using the above properties on the radii of $\mathbb{BT}$ we obtain that

$$2r = w = {}^3\!/_4 D = {}^3\!/_4 \sqrt{2 + {}^{\sqrt{7}}\!/_2}\, R.$$

Hence

$$f(\mathbb{BT}) = \left({}^3\!/_8\sqrt{2 + {}^{\sqrt{7}}\!/_2},\ {}^3\!/_8\sqrt{2 + {}^{\sqrt{7}}\!/_2},\ {}^1\!/_2\sqrt{2 + {}^{\sqrt{7}}\!/_2}\right),$$

and one may easily check that it fulfills the inequalities (lb_1), (lb_2), and (lb_3) with equality.

Denoting the convex hull of p^1, p^2, p^3 and B by $\mathbb{BT}_{\min}$, it holds $f(K) = f(\mathbb{BT})$, iff $\mathbb{BT}_{\min} \subset K \subset \mathbb{BT}$ (cf. Figure 4(b)).

$\mathbb{H}$ The last vertex satisfies (lb_1), (ib_2) and (lb_3) with equality, whereby its shape is determined as follows: from (lb_1) there must exist two parallel lines supporting the inball of the set and because of (ib_2) it must have concentric in- and circumball. The two parallels supporting the inball contain two separated arcs of the circumsphere between them. Let p^1, p^2, p^3 be points, s. t. p^2 and p^3 lie in one arc and each in one of the supporting lines, while p^1 lies in the other arc and equidistant from p^2 and p^3. Finally, we connect p^2 and p^3 by a circular arc centered at p^1, its radius and the radius of the inball chosen, s. t. the arc is tangent to the inball (cf. Figure 5). The convex set bounded by the two supporting parallel lines and the three arcs with centers p^1, p^2, p^3 and radius $\|p^1 - p^2\|$ is called the *hood* and denoted by $\mathbb{H}$.

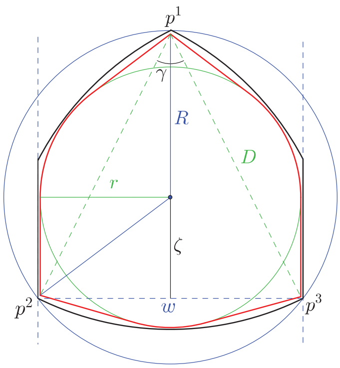

Figure 5: *The hood* $\mathbb{H}$ *in black and* $\mathbb{H}_{\min}$ *in red.*

Recall that we always assume 0 to be the circumcenter and let γ be s. t. $\mathrm{I}_\gamma = \operatorname{conv}\{p^1, p^2, p^3\}$ is the isosceles triangle built by p^1, p^2, p^3, where γ denotes the angle between the two edges of equal length. Thus $R(\mathbb{H}) = R(\mathrm{I}_\gamma)$, $D(\mathbb{H}) = D(\mathrm{I}_\gamma) = r(\mathbb{H}) + R(\mathbb{H})$ and $2r(\mathbb{H}) = w(\mathbb{H})$. For the computation of $r(\mathbb{H})$ let ζ denote the distance from 0 to $[p^2, p^3]$. Considering the two right-angled triangles $\operatorname{conv}\left\{0, p^2, {}^1\!/_2\,(p^2 + p^3)\right\}$ and $\operatorname{conv}\left\{p^1, p^2, {}^1\!/_2\,(p^2 + p^3)\right\}$ we obtain that

$$\text{(i)} \quad r(\mathbb{H})^2 + \zeta^2 = R(\mathbb{H})^2 \qquad \text{and} \qquad \text{(ii)} \quad D(\mathbb{H})^2 = (\zeta + R(\mathbb{H}))^2 + r(\mathbb{H})^2$$

(cf. Figure 5).

Solving (i) for ζ and inserting it into (ii), taking into account that $D(\mathbb{H}) = r(\mathbb{H}) +$

$R(\mathbb{H})$, we obtain that

$$(r(\mathbb{H})+R(\mathbb{H}))^2 = D(\mathbb{H})^2 = (\sqrt{R(\mathbb{H})^2 - r(\mathbb{H})^2} + R(\mathbb{H}))^2 + r(\mathbb{H})^2.$$

Solving for $r(\mathbb{H})$ gives the unique positive real solution

$$r(\mathbb{H}) = \left(\frac{1}{2}\sqrt{\varsigma+\xi} + \sqrt{-\varsigma-\xi+\frac{16}{\sqrt{\varsigma+\xi}}} - 1\right) R(\mathbb{H}),$$

where $\varsigma = 1/3\,(864-96\sqrt{69})^{1/3}$ and $\xi = 2(2/3)^{2/3}(9+\sqrt{69})^{1/3}$. Thus

$$f(\mathbb{H}) = (r(\mathbb{H}), r(\mathbb{H}), 1/2(r(\mathbb{H})+1)) \approx (0.7935, 0.7935, 0.8967).$$

Denoting the convex hull of the inball of $\mathbb{H}$ and p^1, p^2, p^3, by $\mathbb{H}_{\min}$, it holds $f(K) = f(\mathbb{H})$, iff $\mathbb{H}_{\min} \subset K \subset \mathbb{H}$ (cf. Figure 5).

Name	Symbol	Approximate Coordinates	$lb_{1,2,3}$ $ib_{1,2,3}$ $ub_{1,2,3}$
Ball	$\mathbb{B}$	$(1,1,1)$	$+--++-+--$
Equilateral triangle	$\mathbb{I}_{\pi/3}$	$(0.5, 0.75, 0.8660)$	$-+---++++$
Line segment	$\mathbb{L}$	$(0,0,1)$	$++-+---\pm+$
Reuleaux triangle	$\mathbb{RT}$	$(0.7321, 0.8660, 0.8660)$	$----+++--$
Right-angled triangle	$\mathbb{I}_{\pi/2}$	$(0.4142, 0.5, 1)$	$---+---++$
Sailing boat	$\mathbb{SB}$	$(0.7071, 0.8536, 1)$	$---+--++-$
Sliced Reuleaux tr.	$\mathbb{SR}$	$(0.7321, 0.8440, 0.8660)$	$--+-++---$
Flattened Reuleaux tr.	$\mathbb{FR}$	$(0.6495, 0.75, 0.8660)$	$-++--+---$
Bent trapezoid	$\mathbb{BT}$	$(0.6836, 0.6836, 0.9114)$	$+++------$
Hood	$\mathbb{H}$	$(0.7935, 0.7935, 0.8967)$	$+-+-+----$

Table 1: *The table lists the planar sets mapped to vertices of the 3-dimensional Blaschke-Santaló diagram, their (approximate) radii, and the inequalities they fulfill with equality (+) or not (−). The ± for the line segment in the (ub_2)-column points out that $\mathbb{L}$ attaining equality is an artefact.*

REMARK 4.1. Considering Table 1 we may observe the following: all inequalities besides (ub_3) are fulfilled with equality by exactly four vertices. Moreover, since all three vertices of (ub_3) also fulfill (ub_2) with equality (and since we will later prove these two inequalities more or less within one proof), we may understand them as one inequality in two parts. Doing so all inequalities are fulfilled by exactly four vertices, a fact which in a polytopal setting would be quite exceptional. (One should mention that, accepting the two inequalities to be a joint one, the right-angled triangle would not be a vertex anymore due to our definition, but nevertheless we think the whole matter is remarkable.)

4.2. Edges of the diagram

Next we give constructions of explicit families of convex sets mapped onto the intersection of two of the facets collected in Section 3. In particular, every family of sets $\{K_t\}_{t\in[t_1,t_2]}$ described, induces a closed curve $f(\{K_t : t \in [t_1,t_2]\})$ in $\mathbb{R}^3$ (which is differentiable again as it has an algebraic parametric description). In our nomenclature they form the edges of the diagram. Each edge is named via its two endpoints, e. g. $(\mathbb{I}_{\pi/3},\mathbb{B})$ denotes the edge between $\mathbb{I}_{\pi/3}$ and $\mathbb{B}$.

$(\mathbb{RT},\mathbb{B})$ It is a well known property that $w(K) = r(K) + R(K) = D(K)$, iff K is of constant width. Thus all *sets of constant width* fulfill (ub_1) and (ib_2) with equality. Essentially all edges with $\mathbb{B}$ as an endpoint are real linear edges of the diagram: because of Lemma 2.1 we may fill the full edge from $\mathbb{RT}$ to $\mathbb{B}$ with *rounded Reuleaux triangles*, i. e. the outer parallel bodies $(1-\lambda)\mathbb{RT}+\lambda\mathbb{B}$, $\lambda \in [0,1]$ of the Reuleaux triangle.

$(\mathbb{L},\mathbb{B})$ Whenever K is *centrally symmetric* it satisfies the equations $D(K) = 2R(K)$ and $w(K) = 2r(K)$. Thus f maps K onto the linear edge formed from the equality cases of (lb_1) and (ib_1). Again, because of Lemma 2.1, the outer parallel bodies $(1-\lambda)\mathbb{L}+\lambda\mathbb{B}$, $\lambda \in [0,1]$, of $\mathbb{L}$ (called *sausages*) already fill the whole edge.

$(\mathbb{SB},\mathbb{B})$ Lemma 2.1 implies that all *rounded sailing boats* $(1-\lambda)\mathbb{SB}+\lambda\mathbb{B}$, $\lambda \in [0,1]$ satisfy the inequalities (ub_1) and (ib_1) with equality and fill the corresponding edge of the diagram.

$(\mathbb{H},\mathbb{B})$ Because of Lemma 2.1 the *rounded hoods* $(1-\lambda)\mathbb{H}+\lambda\mathbb{B}$, $\lambda \in [0,1]$ satisfy the inequalities (lb_1) and (ib_2) with equality and their images through f fill the corresponding edge.

$(\mathbb{L},\mathbb{I}_{\pi/3})$ As defined above, I_γ denotes an *isosceles triangle* with an angle γ between the two edges of equal length (see Figure 6(a)). If $\gamma \in [0, \pi/3]$, the two edges of equal length attain its diameter $D = D(\mathrm{I}_\gamma) = 2R\cos(\gamma/2)$, where $R = R(\mathrm{I}_\gamma) = 1$. Abbreviating also $r = r(\mathrm{I}_\gamma)$ and $w = w(\mathrm{I}_\gamma)$, it was shown in [15] and [19] that

$$\left(2+\sqrt{4-(D/R)^2}\right) r = w \quad \text{and} \quad 2wR = D^2\sqrt{4-(D/R)^2}.$$

Thus one may check that I_γ fulfills (ub_3) and (lb_2) with equality for any $\gamma \in [0, \pi/3]$.

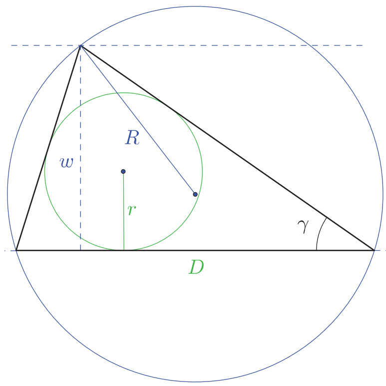

(a) $I_\gamma,\ \gamma \in [0, \pi/3]$.

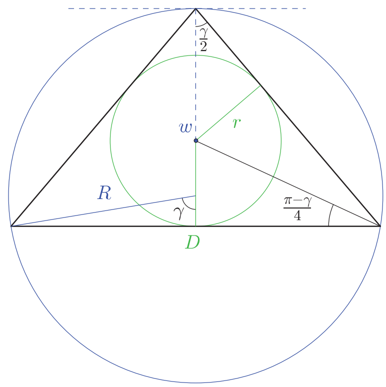

(b) $I_\gamma,\ \gamma \in [\pi/3, \pi/2]$.

Figure 6: *(Acute) isosceles triangles.*

$(\mathbb{I}_{\pi/2}, \mathbb{I}_{\pi/3})$ Consider the family of *isosceles triangles* I_γ as described above, but now with $\gamma \in [\pi/3, \pi/2]$. Obviously their diameter $D(I_\gamma)$ is attained by the edge opposite to γ. Using Lemma 1.3 we obtain that the angle at the circumcenter between the height onto the diametrical edge and the segment between the center and one of the diametrical vertices is again γ (cf. Figure 6(b)). The width is obviously attained orthogonal to the diametrical edge and thus it is the sum of the inradius and the distance from the incenter to the opposing vertex. Considering the right angled triangle with the incenter, the midpoint and one of the endpoints of the diametrical edge as vertices, it is easy to check that the interior angle at that endpoint is $(\pi-\gamma)/4$. Hence $2r(I_\gamma) = D(I_\gamma)\tan((\pi-\gamma)/4)$ and using trigonometric identities it follows

$$\tan\left(\frac{\pi-\gamma}{4}\right) = \frac{1-\cos\left((\pi-\gamma)/2\right)}{\sin\left((\pi-\gamma)/2\right)} = \frac{1-\sin\left(\gamma/2\right)}{\cos\left(\gamma/2\right)} = \frac{1}{\cos(\gamma/2)} - \tan\left(\frac{\gamma}{2}\right).$$

Altogether, omitting arguments we have

$$D = 2R\sin(\gamma), \qquad w = r\left(1+\frac{1}{\sin\left(\gamma/2\right)}\right), \quad \text{and}$$
$$r = \frac{D}{2}\left(\frac{1}{\cos(\gamma/2)} - \tan\left(\frac{\gamma}{2}\right)\right).$$

Finally, again using trigonometric identities, we may remove γ from the width formula in two ways

$$w = r\left(1+\frac{1}{\sin(\gamma/2)}\right) = r\left(1+\sqrt{\frac{2}{1-\cos(\gamma)}}\right)$$
$$= r\left(1+\frac{\sqrt{2}}{\sin(\gamma)}\sqrt{1+\cos(\gamma)}\right) = r\left(1+\frac{2\sqrt{2}R}{D}\sqrt{1+\sqrt{1-\left(\frac{D}{2R}\right)^2}}\right)$$

or

$$= r\left(1+\frac{1}{\sin(\gamma/2)}\right) = 2r\left(1+\frac{1}{2}\left(\frac{1}{\sin(\gamma/2)}-1\right)\right)$$
$$= 2r\left(1+\frac{1/\cos(\gamma/2)-\tan(\gamma/2)}{2\tan(\gamma/2)}\right)$$
$$= 2r\left(1+\frac{r}{D\tan(\gamma/2)}\right) = 2r\left(1+\frac{r(1+\cos(\gamma))}{D\sin(\gamma)}\right)$$
$$= 2r\left(1+\frac{2rR}{D^2}\left(1+\sqrt{1-\left(\frac{D}{2R}\right)^2}\right)\right)$$

proving that $\mathrm{I}_\gamma,\ \gamma \in [\pi/3, \pi/2]$ is extreme for (ub_2) and (ub_3).

$(\mathbb{L}, \mathbb{I}_{\pi/2})$ The next family we consider are the *right-angled triangles* $\mathrm{T}_r^{\pi/2}$, where $r \in [0, r(\mathbb{I}_{\pi/2})]$ denotes their inradius. Naming the lengths of their edges a, b and

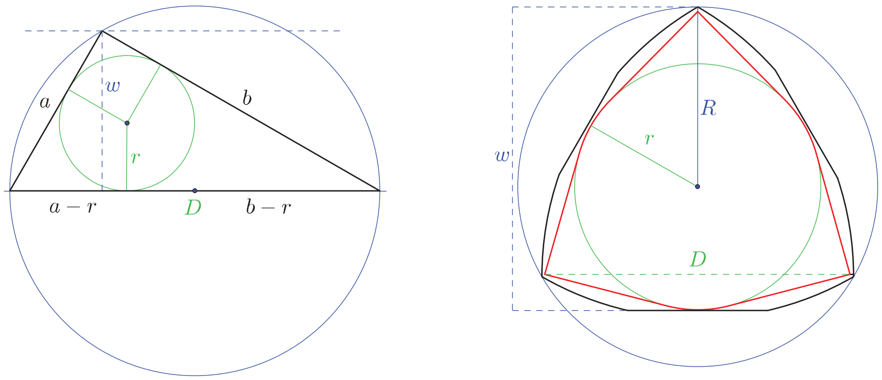

(a) $\mathrm{T}_r^{\pi/2}$.

(b) *In black* RB_r *and in red a Yamanouti set with the same radii.*

Figure 7: *A right-angled triangle and a Reuleaux blossom.*

$D = D(\mathrm{T}_r^{\pi/2}) = 2R(\mathrm{T}_r^{\pi/2})$, abbreviating $w = w(\mathrm{T}_r^{\pi/2})$ and recognizing that the inball touches the diametrical edge, s. t. it is split into two segments of lengths $a-r$ and $b-r$ (see Figure 7(a)), we easily see that the perimeter p of $\mathrm{T}_r^{\pi/2}$ is $2r+2D$ (or $2r+4R$). Thus using the semiperimeter formula for the width, we obtain that

$$wD = 2A = rp = 2r(r+D).$$

One may easily calculate that the right-angled triangles are extreme for the inequalities (ub_3) and (ib_1).

$(\mathbb{I}_{\pi/3}, \mathbb{RT})$ For any $r \in [r(\mathbb{I}_{\pi/3}), r(\mathbb{RT})]$ we call $\mathrm{RB}_r = \left({}^{r}/_{r(\mathbb{I}_{\pi/3})}\mathbb{I}_{\pi/3}\right) \cap \mathbb{RT}$ a *Reuleaux blossom*, s. t. $\mathrm{RB}_{r(\mathbb{I}_{\pi/3})} = \mathrm{RB}_{1/2} = \mathbb{I}_{\pi/3}$ and $\mathrm{RB}_{r(\mathbb{RT})} = \mathrm{RB}_{\sqrt{3}-1} = \mathbb{RT}$ (see Figure 7(b)). Obviously $r(\mathrm{RB}_r) = r$, $D(\mathrm{RB}_r) = \sqrt{3}R(\mathrm{RB}_r)$, and $w(\mathrm{RB}_r) = r + R(\mathrm{RB}_r)$. Hence the Reuleaux blossoms are extreme for the inequalities (ub_1) and (ib_3).

A *Yamanouti set* of inradius r is mapped onto the same coordinates in the 3-dimensional Blaschke-Santaló diagram as the Reuleaux blossom RB_r. They are the convex hull of $\mathbb{I}_{\pi/3}$ and the intersection of three balls with centers in the vertices of $\mathbb{I}_{\pi/3}$ and radius taken in $[w(\mathbb{I}_{\pi/3}), w(\mathbb{RT})]$ (see [19] and cf. Figure 7(b)). While the Yamanouti set is a unique minimal set (with respect to set inclusion) mapped to these coordinates, the corresponding Reuleaux blossom is maximal but not unique (as one may support the inball in different points than the chosen ones). However, the Reuleaux blossoms are the only maximizers which possess the same symmetry group as $\mathbb{I}_{\pi/3}$.

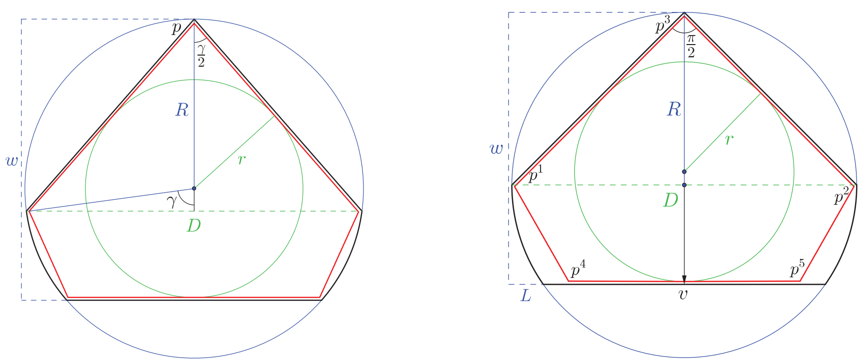

(a) *In black* $\mathrm{SB}_\gamma^{\circledcirc}$, *in red the pentagon* $\mathrm{CP}_\gamma^{\circledcirc}$.

(b) *In black* $\mathrm{SB}_{r,\pi/2}$, *in red the pentagon* $\mathrm{SB}_{r,\pi/2}^{\min}$ *for the case that* $w(\mathrm{SB}_{r,\pi/2}) > \sqrt{2}R(\mathrm{SB}_{r,\pi/2})$.

Figure 8: *A concentric and a right-angled sailing boat.*

$(\mathbb{I}_{\pi/3},\mathbb{SB})$ Let $\gamma \in [\pi/3, \pi/2]$ and c the incenter of I_γ. Now rescale $\mathrm{I}_\gamma - c$ by a factor ρ, s.t. the vertex p of $\rho(\mathrm{I}_\gamma - c)$ between the two edges of equal length touches the boundary of $\mathbb{B}$. Then the *concentric sailing boat* is defined as $\mathrm{SB}_\gamma^{\circledcirc} = \rho(\mathrm{I}_\gamma - c) \cap \mathbb{B}$ (see Figure 8(a)). Obviously, $R = R(\mathrm{SB}_\gamma^{\circledcirc}) = 1$ and $D = D(\mathrm{SB}_\gamma^{\circledcirc}) = D(\mathrm{I}_\gamma) = R\sin(\gamma)$. Moreover, since $\mathrm{SB}_\gamma^{\circledcirc}$ is concentric and the distance of the center from p is R we obtain that

$$r = r(\mathrm{SB}_\gamma^{\circledcirc}) = R\sin\left(\frac{\gamma}{2}\right) \quad \text{and} \quad w = r + R = r\left(1 + \frac{1}{\sin(\gamma/2)}\right).$$

However, since $D = R\sin(\gamma)$ it follows exactly by the same argument as for $w(\mathrm{I}_\gamma)$ in the $(\mathbb{I}_{\pi/3}, \mathbb{I}_{\pi/2})$-edge that

$$w = r\left(1 + \frac{1}{\sin(\gamma/2)}\right) = 2r\left(1 + \frac{2rR}{D^2}\left(1 + \sqrt{1 - \left(\frac{D}{2R}\right)^2}\right)\right).$$

Hence the concentric sailing boats are extreme for the inequalities (ub_1) and (ub_2). Denoting the concentric pentagon built from the vertices of $\mathrm{SB}_\gamma^{\circledcirc}$ by $\mathrm{CP}_\gamma^{\circledcirc}$, it holds $f(K) = f(\mathrm{SB}_\gamma^{\circledcirc})$, iff $\mathrm{CP}_\gamma^{\circledcirc} \subset K \subset \mathrm{SB}_\gamma^{\circledcirc}$ (cf. Figure 8(a)).

$(\mathbb{I}_{\pi/2},\mathbb{SB})$ Let $r \in [r(\mathbb{I}_{\pi/2}), r(\mathbb{SB})]$ and $v \in \mathbb{R}^2$ be s.t. the vertex of $v + ({}^{r}/_{r(\mathbb{I}_{\pi/2})})\mathbb{I}_{\pi/2}$ between the two edges of equal length belongs to $\mathbb{S}$ and the edges of equal length induce equal caps in $\mathbb{B}$ (cf. Figure 8(b)). Then $\mathrm{SB}_{r,\pi/2} = (v + ({}^{r}/_{r(\mathbb{I}_{\pi/2})})\mathbb{I}_{\pi/2}) \cap \mathbb{B}$ is a *right-angled sailing boat*. Hence $D(\mathrm{SB}_{r,\pi/2}) = 2R(\mathrm{SB}_{r,\pi/2})$, $r(\mathrm{SB}_{r,\pi/2}) = r(v + ({}^{r}/_{r(\mathbb{I}_{\pi/2})})\mathbb{I}_{\pi/2}) = r$, and $w(\mathrm{SB}_{r,\pi/2}) = {}^{r}/_{r(\mathbb{I}_{\pi/2})} w(\mathbb{I}_{\pi/2}) = (\sqrt{2}+1)r$. Thus right-angled sailing boats are extreme for the inequalities (ub_2) and (ib_1) and it holds $K \subset \mathrm{SB}_{r,\pi/2}$ for any set K with $f(K) = f(\mathrm{SB}_{r,\pi/2})$. Concerning possible minimal sets mapped to the same coordinates in the diagram, let $p^1, p^2, p^3 \in \mathbb{S}$ be s.t. $\mathrm{conv}\{p^1, p^2, p^3\} = \mathbb{I}_{\pi/2}$, with the right-angle at p^3. Now, if $w(\mathrm{SB}_{r,\pi/2}) \leqslant \sqrt{2}R(\mathrm{SB}_{r,\pi/2})$, the set $\mathrm{SB}_{r,\pi/2}^{\min} := \mathrm{conv}\left(\mathbb{I}_{\pi/2}, (p^3 + w(\mathrm{SB}_{r,\pi/2})\mathbb{B}) \cap \mathrm{SB}_{r,\pi/2}\right)$ fulfills $\mathrm{SB}_{r,\pi/2}^{\min} \subset K$, for all K with $f(K) = f(\mathrm{SB}_{r,\pi/2})$. In case of $w(\mathrm{SB}_{r,\pi/2}) > \sqrt{2}R(\mathrm{SB}_{r,\pi/2})$ (i.e. $r > (2-\sqrt{2}) R(\mathrm{SB}_{r,\pi/2})$), let L be the supporting line to the inball in v, and let $p^4, p^5 \in L$ be at distance $w(\mathrm{SB}_{r,\pi/2})$ from the segments $[p^1, p^3]$ and $[p^2, p^3]$, respectively. Then the pentagon $\mathrm{SB}_{r,\pi/2}^{\min} := \mathrm{conv}\{p^i, i \in [5]\}$ is a minimal set mapped to the same coordinates as $\mathrm{SB}_{r,\pi/2}$. However, one should recognize that $\mathrm{SB}_{r,\pi/2}^{\min}$ is only one (maybe the "nicest") possible choice for such a set (cf. Figure 8(b)).

$(\mathbb{I}_{\pi/3},\mathbb{FR})$ For any $r \in [r(\mathbb{I}_{\pi/3}), r(\mathbb{FR})]$ there exists $c \in \mathbb{R}^2$, s.t. $c + r\mathbb{B}$ is contained in $\mathbb{FR}$ (by the definition of the inradius) and tangent to the linear edge of $\mathbb{FR}$ (cf. Figure 9). Assuming c to be equidistant from the endpoints of that linear edge, the sets $\mathrm{BI}_{r,\pi/3} = \mathrm{conv}(\mathbb{I}_{\pi/3}, v + r\mathbb{B})$, $r \in [r(\mathbb{I}_{\pi/3}), r(\mathbb{FR})]$ are called *bent* *equilaterals* and they satisfy $r(\mathrm{BI}_{r,\pi/3}) = r$, $D(\mathrm{BI}_{r,\pi/3}) = \sqrt{3}R(\mathrm{BI}_{r,\pi/3})$ and $w(\mathrm{BI}_{r,\pi/3}) = w(\mathbb{I}_{\pi/3})$. Thus the bent equilaterals with $r \in [r(\mathbb{I}_{\pi/3}), r(\mathbb{FR})]$ are extreme for the inequalities (lb_2) and (ib_3).

With respect to set inclusion $\mathrm{BI}_{r,\pi/3}$ is a minimal set mapped onto these coordinates. However, since there is some freedom in placing c, it is not a unique minimal set.

Choosing two common supporting halfspaces H_i with $\mathrm{bd}(H_i) = L_i$, $i = 1,2$, of $\mathrm{BI}_{r,\pi/3}$ and its inball, s. t. $c + r\mathbb{B}$ is the inball of $\mathbb{FR} \cap H_1 \cap H_2$, one gets a maximal set containing $\mathrm{BI}_{r,\pi/3}$ (but neither the choice of the halfspaces H_i, $i = 1,2$ is unique nor is the choice of c, cf. Figure 9).

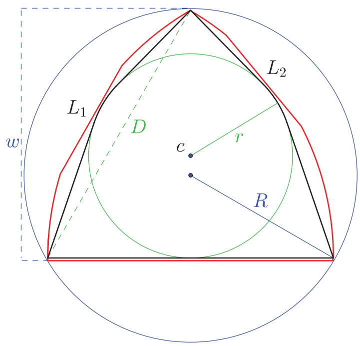

Figure 9: *In black a bent equilateral* $\mathrm{BI}_{r,\pi/3}$, $r \in [r(\mathbb{I}_{\pi/3}), r(\mathbb{FR})]$ *(for which all radii keep constant moving the inball horizontally), in red one possible maximal set containing* $\mathrm{BI}_{r,\pi/3}$.

($\mathbb{FR}, \mathbb{SR}$) On the contrary, for any $r \in [r(\mathbb{FR}), r(\mathbb{SR})]$, let $c \in \mathbb{R}^2$ be s. t. $c + r\mathbb{B}$ is tangent to the two (non-linear) arcs of $\mathbb{FR}$ (see Figure 10(b)). Then we define the *maximally-sliced Reuleaux triangle* SR_{r,w_r} as follows: take the intersection of $\mathbb{RT}$ with a halfspace supporting $c + r\mathbb{B}$ and containing a vertex of $\mathbb{FR}$, which is adjacent to its linear edge, on the boundary line of the halfspace. Abbreviating $D = D(\mathrm{SR}_{r,w_r})$ and $R = R(\mathrm{SR}_{r,w_r}) = 1$ again, it holds $r(\mathrm{SR}_{r,w_r}) = r$ and $D = \sqrt{3}R$. Considering the angles α, β, γ inside SR_{r,w_r} (as given in Figure 10(b)), we have

(i) $\cos(\alpha) = {}^{D}/_{2(D-r)}$, (ii) $\sin(\alpha+\beta) = {}^{r}/_{(D-r)}$, (iii) $\cos(\gamma) = {}^{w}/_{D}$.

Passing (i) into (ii) one obtains that

$$\beta = \arcsin\left(\frac{r}{D-r}\right) - \arccos\left(\frac{D}{2(D-r)}\right)$$

and since $\gamma = {}^{\pi}/_{6} - \beta$ it follows from (iii) for the width $w = w(\mathrm{SR}_{r,w_r})$ that

$$w = D\cos\left(\frac{\pi}{6} - \arcsin\left(\frac{r}{D-r}\right) + \arccos\left(\frac{D}{2(D-r)}\right)\right).$$

The sliced Reuleaux triangles fulfill the inequalities (lb_3) and (ib_3) with equality. Moreover, calling $\mathrm{BI}_{r,\pi/3} := \mathrm{conv}(\mathbb{I}_{\pi/3}, c + r\mathbb{B})$, with $r \in [r(\mathbb{FR}), r(\mathbb{SR})]$ again a *bent equilateral*, it holds $f(K) = f(\mathrm{SR}_{r,w_r})$, iff $\mathrm{BI}_{r,\pi/3} \subset K \subset \mathrm{SR}_{r,w_r}$ (cf. Figure 10(b)).

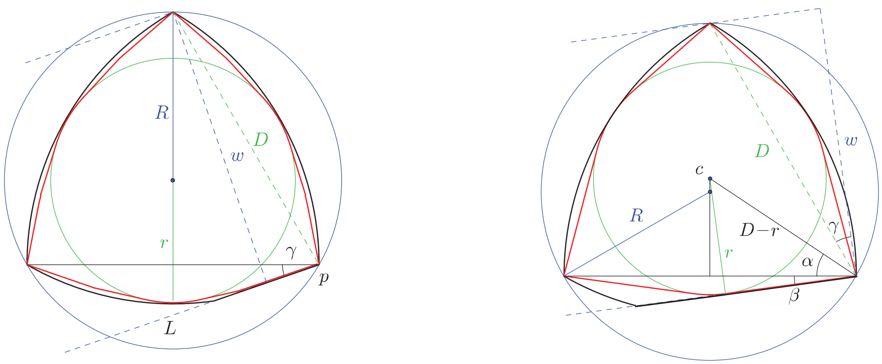

(a) *In black a concentric sliced Reuleaux triangle* $\mathrm{SR}^{\circledcirc}_{\gamma}$ *and in red* BY_{γ}.

(b) *In black a maximally-sliced Reuleaux triangle* SR_{r,w_r}, *in red a bent equilateral* $\mathrm{BI}_{r,\pi/3}$, $r \in [r(\mathbb{FR}), r(\mathbb{SR})]$.

Figure 10: *Sliced Reuleaux triangles*

($\mathbb{SR}, \mathbb{RT}$) Let L be a line containing a vertex of $\mathbb{RT}$, say p, not cutting the interior of the inball of $\mathbb{RT}$. Then consider the angle $\gamma \in [\arcsin(\sqrt{3}-1) - \pi/6, \pi/6]$ between L and one of the segments joining p with one of the other two vertices (see Figure 10(a)). The family of *concentric sliced Reuleaux triangles* $\mathrm{SR}^{\circledcirc}_{\gamma}$ is obtained from intersecting $\mathbb{RT}$ with the halfspace induced by L. The concentric sliced Reuleaux triangles have the same diameter, in-, and circumradius as $\mathbb{RT}$, while the width is attained orthogonally to the line L. Hence $w(\mathrm{SR}^{\circledcirc}_{\gamma}) = D(\mathbb{RT}) \sin(\pi/3 + \gamma)$. Concentric sliced Reuleaux triangles are extreme for the inequalities (ib_2) and (ib_3).

Denoting the convex hull of $r(\mathrm{SR}^{\circledcirc}_{\gamma})\mathbb{B}$ and the Yamanouti set sharing the same width, diameter and circumradius with $\mathrm{SR}^{\circledcirc}_{\gamma}$ by BY_{γ}, we obtain $f(K) = f(\mathrm{SR}^{\circledcirc}_{\gamma})$, iff $\mathrm{BY}_{\gamma} \subset K \subset \mathrm{SR}^{\circledcirc}_{\gamma}$ (see Figure 10(a)).

($\mathbb{L}, \mathbb{BT}$) The construction of the sets in the edge ($\mathbb{L}, \mathbb{BT}$) is a generalization of that of the bent trapezoid $\mathbb{BT}$ in Subsection 4.1. Let $\mathrm{I}_{\gamma} = \mathrm{conv}\{p^1, p^2, p^3\}$ with $\gamma \in [0, \arcsin(3/4)]$ be s. t. γ is the angle at p^1. Moreover, let $p^4 \neq p^3$ in the circumsphere of I_{γ} be s. t. $\mathrm{conv}\{p^1, p^2, p^4\}$ is congruent to $\mathrm{conv}\{p^1, p^2, p^3\}$ and possesses its angle γ at p^2. Substituting the two edges $[p^1, p^4]$ and $[p^2, p^3]$ by two arcs of radius $D(\mathrm{I}_{\gamma})$ with centers in p^1 and p^2, respectively, the resulting set is a *(general) bent trapezoid* BT_{γ}, $\gamma \in [0, \arcsin(3/4)]$ (see Figure 11(a)). It holds $D(\mathrm{BT}_{\gamma}) = D(\mathrm{I}_{\gamma}) = 2R(\mathrm{I}_{\gamma}) \cos(\gamma/2)$ and $w(\mathrm{BT}_{\gamma}) =$

$w(\mathrm{I}_\gamma) = D(\mathrm{I}_\gamma)\sin(\gamma)$ and since they possess two parallel edges touching the inball in antipodal points we have $w(\mathrm{BT}_\gamma) = 2r(\mathrm{BT}_\gamma)$.

The bent trapezoids are extreme for the inequalities (lb_1) and (lb_2). While BT_γ is the unique maximal set with respect to set inclusion, which is mapped onto these coordinates in the diagram, there does not exist a unique minimal set. Essentially, the convex hull of I_γ and any of the possible inballs of BT_γ shares all four radii with BT_γ and is minimal in that sense.

($\mathbb{BT},\mathbb{FR}$) Adopting the construction of the bent trapezoids with $\gamma \in [0, \arcsin(3/4)]$ above, we define the *(general) bent trapezoid* BT_γ with $\gamma \in [\arcsin(3/4), \pi/3]$ (see Figure 11(a)). Bent trapezoids with $\gamma > \arcsin(3/4)$ still fulfill $D(\mathrm{BT}_\gamma) = D(\mathrm{I}_\gamma) = 2R(\mathrm{I}_\gamma)\cos(\gamma/2)$, and $w(\mathrm{BT}_\gamma) = w(\mathrm{I}_\gamma) = D(\mathrm{I}_\gamma)\sin(\gamma)$, but in difference to the bent trapezoids with $\gamma < \arcsin(3/4)$, the ones with $\gamma \geqslant \arcsin(3/4)$ have an inball touching the two diametrical arcs and only the longer of the parallels. Thus it holds $1/4 D(\mathrm{BT}_\gamma)^2 + r(\mathrm{BT}_\gamma)^2 = (D(\mathrm{BT}_\gamma) - r(\mathrm{BT}_\gamma))^2$ from which we obtain that $3/4 D(\mathrm{BT}_\gamma)^2 - 2D(\mathrm{BT}_\gamma)r(\mathrm{BT}_\gamma) = 0$ or $8r(\mathrm{BT}_\gamma) = 3D(\mathrm{BT}_\gamma)$. Hence the sets BT_γ, $\gamma \in [\arcsin(3/4), \pi/3]$, fulfill inequalities ($lb_2$) and ($lb_3$) with equality.

BT_γ is the unique maximal set with respect to set inclusion. The bent isosceles given by the convex hull of one of the two possible copies of I_γ inside BT_γ and the inball of BT_γ is a minimal set with respect to set inclusion mapped to the same coordinates (see Subsection 4.3 for details about bent isosceles). It is unique up to mirroring along the symmetry axis of BT_γ, cf. Figure 11(b).

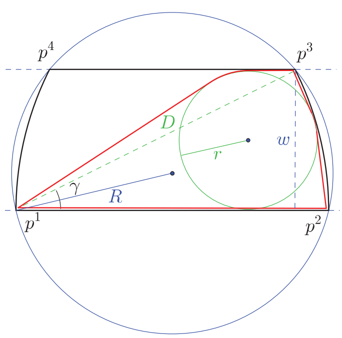

(a) *In black* BT_γ *with* $\gamma < \arcsin(3/4)$, *in red a minimal set whose inball is tangent to one of the curved edges of* BT_γ.

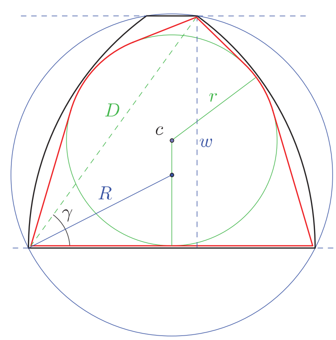

(b) *In black* BT_γ *with* $\gamma > \arcsin(3/4)$, *in red a corresponding bent isosceles.*

Figure 11: *Bent trapezoids.*

($\mathbb{SR},\mathbb{H}$) Now, we generalize the hood $\mathbb{H}$ as constructed in Subsection 4.1: For any $\gamma \in [2\arcsin(r(\mathbb{H})/D(\mathbb{H})), \pi/3]$ let $\mathrm{I}_\gamma = \mathrm{conv}\{p^1, p^2, p^3\}$ be, s. t. $D(\mathrm{I}_\gamma) = \|p^1 - p^2\| = \|p^1 - p^3\|$. Then we define the area contained between

- the arcs with centers in the vertices of I_γ and radius $D(\mathrm{I}_\gamma)$,
- the line L, passing through p^2, supporting the ball $\big(D(\mathrm{I}_\gamma)-R(\mathrm{I}_\gamma)\big)\mathbb{B}$, and possessing the smaller angle β between it and $[p^1,p^2]$, as well as
- the parallel line L' to L supporting I_γ in p^3,

as the *(general) hood* H_γ (see Figure 12(a)).

One can easily see that $D(\mathrm{H}_\gamma)=D(\mathrm{I}_\gamma)=2R(\mathrm{I}_\gamma)\cos(\gamma/2)$ and $r(\mathrm{H}_\gamma)=D(\mathrm{H}_\gamma)-R(\mathrm{H}_\gamma)$.

Observe that the angle between $[p^1,p^2]$ and $[0,p^2]$ in p^2 is $\gamma/2$. Now, let α be the angle between $[p^2,p^3]$ and the perpendicular of L in p^2 and let $\beta=\gamma/2-\alpha$ be the angle between $[p^1,p^2]$ and L in p^2. Then, omitting the argument H_γ, we obtain

$$\text{(i)}\quad D=2R\cos(\gamma/2),\qquad \text{(ii)}\quad r=R\sin(\gamma/2+\beta)=R\sin(\gamma-\alpha),$$
$$\text{(iii)}\quad w=\left\|p^2-p^3\right\|\cos(\alpha)=2D\sin(\gamma/2)\cos(\alpha).$$

From (i) and (ii) one immediately gets that $\gamma/2=\arccos(D/2R)$ and that $\alpha=\gamma-\arcsin(r/R)$. Thus (iii) can be rewritten as

$$\begin{aligned} w &= 2D\sin(\arccos(D/2R))\cos(\gamma-\arcsin(r/R)) \\ &= 2D\sqrt{1-\left(\frac{D}{2R}\right)^2}\cos\left(2\arccos\left(\frac{D}{2(D-r)}\right)-\arcsin\left(\frac{r}{D-r}\right)\right). \end{aligned}$$

The hoods H_γ with $\gamma\in[2\arcsin(r(\mathbb{H})/D(\mathbb{H})),\pi/3]$ are extreme for the inequalities (lb_3) and (ib_2). While H_γ is maximal with respect to set inclusion, the bent isosceles $\operatorname{conv}(\mathrm{I}_\gamma,(D(\mathrm{H}_\gamma)-R(\mathrm{H}_\gamma))\mathbb{B})$ is minimal sharing all radii with H_γ (see Figure 12(a)).

($\mathbb{BT},\mathbb{H}$) Let $r\in[r(\mathbb{BT}),r(\mathbb{H})]$ and γ_r be the maximal $\gamma\in[0,\pi/3]$ s. t. we can find $c\in\mathbb{R}^2$ for which

(i) $c+r\mathbb{B}$ is tangent to the two arcs with centers p^1 and p^2 and radius $D(\mathrm{I}_{\gamma_r})$ above the segments $[p^2,p^3]$ and $[p^1,p^3]$, respectively, as well as

(ii) two parallel lines L and L', which both support $c+r\mathbb{B}$, also support I_{γ_r} in p^2 and p^3, respectively (cf. Figure 12(b)).

The *bent pentagon* BP_{r,γ_r} is defined as the area contained between the lines L,L' and the three arcs with radius $D(\mathrm{I}_{\gamma_r})$ centered in the vertices of I_{γ_r}. These bent pentagons satisfy $D(\mathrm{BP}_{r,\gamma_r})=D(\mathrm{I}_{\gamma_r})=2R(\mathrm{I}_{\gamma_r})\cos(\gamma_r/2)$, $r(\mathrm{BP}_{r,\gamma_r})=r$, and $w(\mathrm{BP}_{r,\gamma_r})=2r(\mathrm{BP}_{r,\gamma_r})$ and are extreme for the inequalities (lb_1) and (lb_3).

Defining the bent isosceles $\mathrm{BI}_{r,\gamma_r}:=\operatorname{conv}(\mathrm{I}_{\gamma_r},c+r\mathbb{B})$ (as we will do in Subsection 4.3), we obtain that $f(K)=f(\mathrm{BP}_{r,\gamma_r})$, iff $\mathrm{BI}_{r,\gamma_r}\subset K\subset\mathrm{BP}_{r,\gamma_r}$.

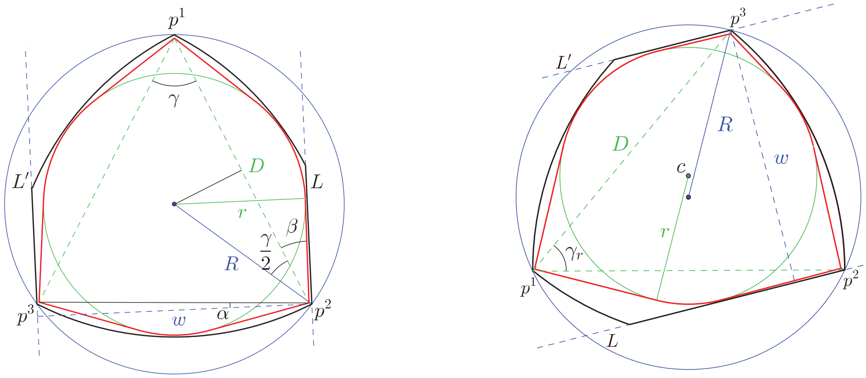

(a) *In black a general hood* H_γ, *in red a bent isosceles.*

(b) *In black a bent pentagon* BP_{r,γ_r} *and in red a bent isosceles* BI_{r,γ_r}, $r \in [r(\mathbb{BT}), r(\mathbb{H})]$.

Figure 12: *Sets from the two edges meeting in* $\mathbb{H}$ *and bounding* (lb_3).

4.3. Facets of the diagram

For each of the inequalities stated in Section 3 we will describe families of sets in $\mathscr{K}^2$, s. t. for every point $x \in [0,1]^3$ in the induced facet of $f(\mathscr{K}^2)$ a set K_x with $f(K_x) = x$ is given.

(lb_1) Due to Lemma 2.1, all outer parallel bodies K, of either the bent trapezoids BT_γ belonging to the $(\mathbb{L}, \mathbb{BT})$-edge or the bent pentagons $\mathrm{BP}_{r,\gamma}$ belonging to the $(\mathbb{BT}, \mathbb{H})$-edge, fulfill the equation

$$2r(K) = w(K).$$

This means (lb_1) induces a linear facet of the diagram, which is bounded by the edges $(\mathbb{L}, \mathbb{BT})$ (bent trapezoids with $\gamma \leqslant 3/4$), $(\mathbb{BT}, \mathbb{H})$ (bent pentagons), $(\mathbb{L}, \mathbb{B})$ (sausages) and $(\mathbb{H}, \mathbb{B})$ (rounded hoods).

(ib_1) If K is an outer parallel body of a right-angled triangle $\mathrm{T}_r^{\pi/2}$ or a right-angled sailing-boat $\mathrm{SB}_{r,\pi/2}$ as described in Section 4.2, then Lemma 2.1 ensures

$$D(K) = 2R(K),$$

which means equality in (ib_1). Hence (ib_1) induces a linear facet of the diagram bounded by the edges $(\mathbb{L}, \mathbb{B})$ (sausages), $(\mathbb{L}, \mathbb{I}_{\pi/2})$ (right-angled triangles), $(\mathbb{I}_{\pi/2}, \mathbb{SB})$ (right-angled sailing-boats), and $(\mathbb{SB}, \mathbb{B})$ (rounded sailing boats).

Many more sets are mapped to the two facets induced by (lb_1) and (ib_1). Recall that, e. g., all symmetric sets are mapped to the edge obtained from the intersection of the two facets.

(ub_1) Due to Lemma 2.1 any outer parallel body K of a Reuleaux blossom RB_r or of a concentric sailing boat $\mathrm{SB}_\gamma^{\circledcirc}$ fulfills $w(K)=r(K)+R(K)$. Moreover, if K^* is a Scott-completion of a concentric sailing boat $\mathrm{SB}_\gamma^{\circledcirc}$, we obtain from Lemma 2.3 that any of the sets $K_\lambda := \lambda K + (1-\lambda)K^*$, $\lambda \in [0,1]$, fulfills $w(K)=r(K)+R(K)$, too. Thus (ub_1) defines a linear facet of the diagram, bounded by the edges $(\mathbb{I}_{\pi/3},\mathbb{RT})$ (Reuleaux blossoms) and $(\mathbb{RT},\mathbb{B})$ (rounded Reuleaux triangles), as well as $(\mathbb{I}_{\pi/3},\mathbb{SB})$ (concentric sailing boats) and $(\mathbb{SB},\mathbb{B})$ (rounded sailing boats).

(ib_2) Lemma 2.1 ensures that any outer parallel body K of a general hood H_γ or of a concentric sliced Reuleaux triangle $\mathrm{SR}_\gamma^{\circledcirc}$ fulfills

$$D(K)=r(K)+R(K).$$

Thus we obtain a filling of the linear facet plainly from the star-shapedness with respect to $\mathbb{B}$. In addition, if K is a set from the edges $(\mathbb{SR},\mathbb{H})$ or $(\mathbb{H},\mathbb{B})$ and K^* a corresponding Scott-completion, then, by Lemma 2.3, the sets $K_\lambda := \lambda K + (1-\lambda)K^*$, $\lambda \in [0,1]$, fulfill $D(K)=r(K)+R(K)$ too. Hence using Lemma 2.3, we obtain a filling of the facet in horizontal lines with respect to the inradius-axis.

Either way we see that (ib_2) induces the fourth linear facet. Its boundary edges are $(\mathbb{SR},\mathbb{H})$ (general hoods), $(\mathbb{H},\mathbb{B})$ (rounded hoods), $(\mathbb{SR},\mathbb{RT})$ (concentric sliced Reuleaux triangles), and $(\mathbb{RT},\mathbb{B})$ (rounded Reuleaux triangles).

(ib_3) As shown in [16] a set $K \in \mathscr{K}^2$ fulfills

$$D(K)=\sqrt{3}R(K),$$

iff K contains an equilateral triangle $\mathbb{I}_{\pi/3}$ of the same circumradius. Since $\mathbb{RT}$ is the unique Scott-completion of $\mathbb{I}_{\pi/3}$, we obtain that $\mathbb{I}_{\pi/3} \subset K \subset \mathbb{RT}$.

Consider a Reuleaux blossom $\mathrm{RB}_r = 2r\mathbb{I}_{\pi/3} \cap \mathbb{RT}$ with $r \in [r(\mathbb{I}_{\pi/3}), r(\mathbb{RT})]$. We describe a continuous transformation of RB_r, keeping the inradius, diameter and circumradius constant and decreasing the width until it becomes a set from the edge $(\mathbb{I}_{\pi/3},\mathbb{FR})$ or $(\mathbb{FR},\mathbb{SR})$. Let p^i, $i=1,2,3$ be s. t. $\mathbb{I}_{\pi/3}=\mathrm{conv}\{p^1,p^2,p^3\}$. While the transformation ending in the sets from the edge $(\mathbb{I}_{\pi/3},\mathbb{FR})$ can be done within one step (Step (i) below), the transformation of the sets which should approach the edge $(\mathbb{FR},\mathbb{SR})$ must be done in two steps (Step (i) and (ii) below):

(i) We translate $2r\mathbb{I}_{\pi/3}$ in direction of p^1, until either its inball becomes tangent to $[p^2,p^3]$ (when $r(\mathbb{I}_{\pi/3}) \leqslant r \leqslant r(\mathbb{FR})$) or tangent to both arcs of $\mathbb{RT}$ intersecting in p^1 (when $r(\mathbb{FR}) \leqslant r \leqslant r(\mathbb{SR})$, see Figure 13(a)). We define the *(non-concentric) Reuleaux blossom* by $\mathrm{RB}_{r,v} := (v+2r\mathbb{I}_{\pi/3}) \cap \mathbb{RT}$, where v is a point on the segment $[0,tp^1]$ with $0 \leqslant t < 1$ chosen, s. t. in case of $v=tp^1$ one of the two stopping reasons for the translation is reached (cf. Figure 13(a)).

Observe that when $r(\mathbb{I}_{\pi/3}) \leqslant r \leqslant r(\mathbb{FR})$ all radii of RB_{r,tp^1} coincide with the ones of a bent equilateral $\mathrm{BI}_{r,\pi/3}$ (cf. Figure 9), which means that we finished the transformation.

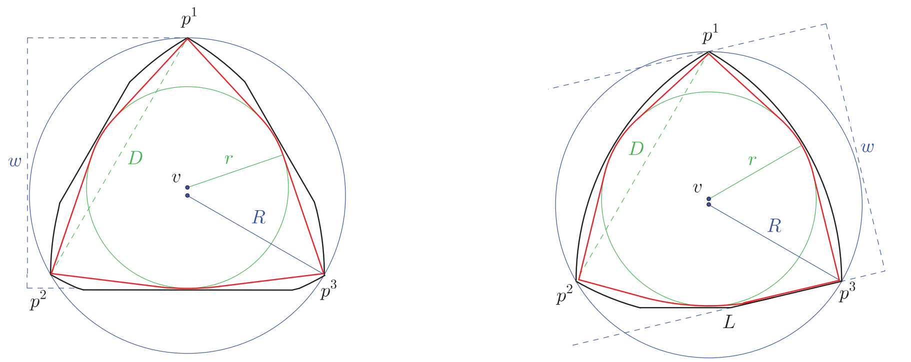

(a) *In black a non concentric Reuleaux blossom and in red the corresponding minimal set.*

(b) *In black a sliced Reuleaux triangle and the corresponding minimal set in red.*

Figure 13: *Examples for the sets, which are maped onto* (ib_3), *corresponding to the cases (i) and (ii) in the description.*

(ii) In case of $r(\mathbb{FR}) \leqslant r \leqslant r(\mathbb{SR})$ the width needs to be further reduced. However, since the tangent lines to the inball do not support the diameter arcs of $\mathbb{RT}$ intersecting in p^1, we first "fill" the area between RB_{r,tp^1} and these arcs, keeping all radii constant, but obtaining a maximal set. Afterwards let L be a line containing p^3 and cutting the extreme Reuleaux blossom RB_{r,tp^1}, s. t. the distance of p^1 and L is the same as the width of RB_{r,tp^1}. Then we rotate L continuously until it becomes tangent to the inball of RB_{r,tp^1} (see Figure 13(b)). Let L^- denote the halfspace bounded by L and containing the inball. Then the set $\mathrm{SR}_{2,r,w} = \mathrm{RB}_{r,tp^1} \cap L^-$ is called a *general sliced Reuleaux triangle*. Finally, when L^- becomes tangent to the inball, we need to "fill" again, this time the complete area of $\mathbb{RT}$ inside L^-.

Observe that in that moment the general sliced Reuleaux triangle reaches the edge $(\mathbb{FR},\mathbb{SR})$, becoming a maximally sliced Reuleaux triangle. Moreover, starting with the Reuleaux triangle the general sliced Reuleaux triangles become concentric sliced Reuleaux triangles and the transformation finally approaches $\mathbb{SR}$.

Both, non-concentric Reuleaux blossoms and general sliced Reuleaux triangles are maximal sets with respect to set inclusion. The *corresponding* minimal sets are the convex hull of $\mathrm{conv}(\mathbb{I}_{\pi/3}, v + r\mathbb{B})$ with the intersection of the three balls centered in the vertices of $\mathbb{I}_{\pi/3}$ and each of radius $w(\mathrm{RB}_{r,v})$ or $w(\mathrm{SR}_{2,r,w})$, depending if we are in case (i) or (ii).

(lb_2) It was shown in [15] that every isosceles I_γ, $\gamma \in [0, \pi/3]$, fulfills

$$(4R(K)^2 - D(K)^2)D(K)^4 = 4w(K)^2R(K)^4$$

with equality. But as already described in [4] they are not the only ones. Since r does not appear in this inequality any superset of an isosceles I_γ keeping the same circumradius, diameter, and width is mapped to the same facet. This is true, e. g. for all bent trapezoids BT_γ on the edges $[\mathbb{L},\mathbb{BT}]$ and $[\mathbb{BT},\mathbb{FR}]$ and surely also for any minimal version $\mathrm{conv}(\mathrm{I}_\gamma, c_\gamma + r(\mathrm{BT}_\gamma)\mathbb{B})$, where c_γ denotes an incenter of BT_γ. Thus choosing any $r \in [r(\mathrm{I}_\gamma), r(\mathrm{BT}_\gamma)]$ and an appropriate incenter c the sets $\mathrm{conv}\left(\mathrm{I}_\gamma, c + r\mathbb{B}\right)$ would have inradius r and the same circumradius, diameter, and width than I_γ and BT_γ (see Figure 14). Let us remark that in many cases the choice of the incenter above will not be unique, as the centers c_γ of $\mathbb{BT}_\gamma$ where not always unique, neither.

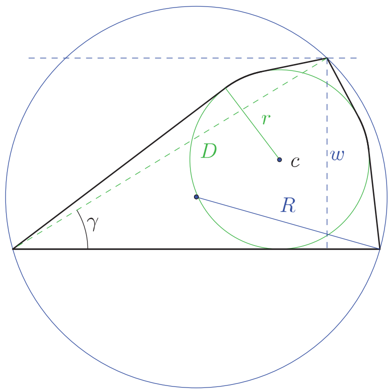

Figure 14: *An example of a minimal set from* (lb_2).

Hence the facet induced by (lb_2) is filled by those sets and bounded by the edges $(\mathbb{L}, \mathbb{I}_{\pi/3})$ (isosceles triangles with $\gamma \in [0, \pi/3]$), $(\mathbb{L}, \mathbb{BT})$, and $(\mathbb{BT}, \mathbb{FR})$ (both kinds of bent trapezoids), as well as by the edge $(\mathbb{I}_{\pi/3}, \mathbb{FR})$ (bent equilaterals with the inball being tangent to an edge of $\mathbb{I}_{\pi/3}$).

One should observe that for any fixed incenter c the sets $\mathrm{conv}\left(\mathrm{I}_\gamma, c + r\mathbb{B}\right)$ are minimal sets with respect to set inclusion mapped to these coordinates in the diagram and are constructed in the same way than the bent isosceles in (lb_3) below.

(lb_3) For any $r \in [0,1]$ and $\gamma \in [0, \pi/3]$ let

(i) $p^1, p^2, p^3 \in \mathbb{S}$ be s. t. $\mathrm{I}_\gamma = \mathrm{conv}\{p^1, p^2, p^3\}$ with $D(\mathrm{I}_\gamma) = \left\|p^1 - p^2\right\| = \left\|p^1 - p^3\right\|$,

(ii) $c \in \mathbb{R}^2$ be s. t. the ball $c + r\mathbb{B}$ is tangent to the two arcs with centers p^1, p^2 and radius $D(\mathrm{I}_\gamma)$,

(iii) L_1 be the one of the two lines containing p^2 and supporting $c + r\mathbb{B}$, possessing the smaller angle with $[p^1, p^2]$, and

(iv) L_2 be the parallel line of L_1 passing through p^3.

Then a *generalized bent pentagon* $\mathrm{BP}_{r,\gamma}$ is defined as the area surrounded by L_1, L_2, and the three arcs of radius $D(\mathrm{I}_\gamma)$ with centers p^1, p^2, and p^3 (see Figure 15).

If we can ensure that $\mathrm{I}_\gamma \subset \mathrm{BP}_{r,\gamma}$, that $c + r\mathbb{B}$ is the inball of $\mathrm{BP}_{r,\gamma}$, and that $w(\mathrm{BP}_{r,\gamma}) = d(L_1, L_2)$, we simply call it a *bent pentagon* (see Figure 15(a)).

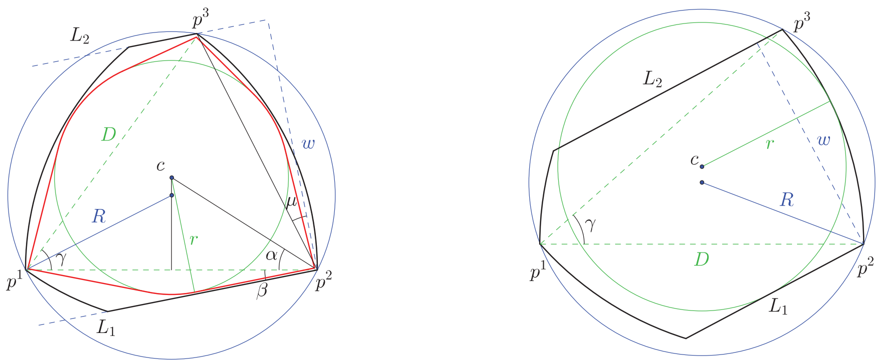

(a) *A bent pentagon* $\mathrm{BP}_{r,\gamma}$ *(black) and a bent isosceles* $\mathrm{BI}_{r,\gamma}$ *(red), the maximal and minimal sets mapped to the same coordinates in* (lb_3).

(b) *A generalized bent pentagon not being a bent pentagon as* $r(\mathrm{BP}_{r,\gamma}) < r$.

Figure 15: *Generalized bent pentagons*

Recall the following edges: the bent trapezoids from $(\mathbb{BT}, \mathbb{FR})$, the bent pentagons from $(\mathbb{BT}, \mathbb{H})$, the maximally-sliced Reuleaux triangles from $(\mathbb{FR}, \mathbb{SR})$, and the general hoods from $(\mathbb{SR}, \mathbb{H})$. It is easy to check from their construction that all of them are particular cases of bent pentagons in the above sense. We will justify why these four edges describe the boundaries of (lb_3) in showing that they bound the range of the parameters r, γ, s. t. a generalized bent pentagon is a bent pentagon. To be more precise, we show that the bent pentagons and the bent trapezoids bound γ from below, while the general hoods and the maximally-sliced Reuleaux triangles bound γ from above.

LEMMA 4.2. *Let* $r \in [0,1]$, $0 \leqslant \gamma < \bar{\gamma} \leqslant \pi/3$, *and let* L_1, L_2 *as well as* $\bar{L}_1, \bar{L}_2$ *be the corresponding parallels in the construction of the generalized bent pentagons* $\mathrm{BP}_{r,\gamma}$ *and* $\mathrm{BP}_{r,\bar{\gamma}}$, *respectively. Then*

a) the ball $c + r\mathbb{B}$, *used in the construction, intersects (is tangent to)* $[p^1, p^2]$, *iff* $8r \geqslant 3D(\mathrm{I}_\gamma)$ $(8r = 3D(\mathrm{I}_\gamma))$.

b) restricting to the case $8r \geqslant 3D(\mathrm{I}_\gamma)$, *it holds that* $d(L_1, L_2) < d(\bar{L}_1, \bar{L}_2)$.

Proof.

a) The distance from c to $[p^1,p^2]$ is at most r, iff $[p^1,p^2]$ intersects $c+r\mathbb{B}$, that is, when $d(c,[p^1,p^2])^2 = (D(\mathrm{BP}_{r,\gamma})-r)^2 - 1/4\,D(\mathrm{BP}_{r,\gamma})^2 \leqslant r^2$ (cf. the right-angled triangle $T=\mathrm{conv}\{c,p^2,1/2\,(p^1+p^2)\}$ in Figure 15(a)). From simplifying we obtain that this is equivalent to $3/4\,D(\mathrm{BP}_{r,\gamma})-2r\leqslant 0$ or $8r\geqslant 3D(\mathrm{BP}_{r,\gamma})$ with equality, iff $r=d(c,[p^1,p^2])$, which means that the inball is tangent to $[p^1,p^2]$.

b) We use the complete notation as in the construction of the bent pentagons, with a bar on top for $\mathrm{BP}_{r,\bar{\gamma}}$ and assume that $[p^1,p^2]$ as well as $[\bar{p}^1,\bar{p}^2]$ are horizontal, below 0 with $p^1_1\leqslant p^2_1$ and $\bar{p}^1_1\leqslant\bar{p}^2_1$. Then it follows from Part (a) that all lines $L_i,\bar{L}_i$, $i=1,2$, have non-negative slope. Since the function $f(x)=(x-r)^2-1/4\,x^2$ is increasing, if $x\geqslant 2r$ it follows

$$d(c,[p^1,p^2]) = \sqrt{(D(\mathrm{BP}_{r,\gamma})-r(\mathrm{BP}_{r,\gamma}))^2-1/4\,D(\mathrm{BP}_{r,\gamma})^2}$$
$$> \sqrt{(D(\mathrm{BP}_{r,\bar{\gamma}})-r(\mathrm{BP}_{r,\bar{\gamma}}))^2-1/4\,D(\mathrm{BP}_{r,\bar{\gamma}})^2} = d(\bar{c},[\bar{p}^1,\bar{p}^2]).$$

Using again the triangle T defined above and the pythagorean theorem, we obtain that

$$p^2_2 = -\sqrt{1-1/4\,D(\mathrm{BP}_{r,\gamma})^2} > -\sqrt{1-1/4\,D(\mathrm{BP}_{r,\bar{\gamma}})^2} = \bar{p}^2_2.$$

Moreover, since $\gamma<\bar{\gamma}$, rotating I_γ around $\mathbb{S}$ until p^1 becomes $\bar{p}^1$, it follows $p^j, j=2,3$ belong to the smaller of the two arcs of $\mathbb{S}$ with endpoints $\bar{p}^j, j=2,3$. Thus in particular it holds $p^3_2<\bar{p}^3_2$ after the rotation. Undoing the rotation, i.e. p^1 moves upward and p^2,p^3 downwards into their old positions, it still holds $p^3_2<\bar{p}^3_2$ and therefore also both points p^2,p^3 still lie in the shorter arc of $\mathbb{S}$ with endpoints $\bar{p}^j, j=2,3$. Now, it follows from $\gamma<\bar{\gamma}$ that $\|p^1-p^2\|>\left\|\bar{p}^1-\bar{p}^2\right\|$, which together with $d(c,[p^1,p^2])>d(\bar{c},[\bar{p}^1,\bar{p}^2])$ means that the slope of L_1 is less than the one of $\bar{L}_1$. Using this fact, we see that if one rotates $\bar{L}_i$, $i=1,2$, around $\bar{p}^i$, $i=2,3$, s.t. they become parallel to L_i, $i=1,2$, their distance decreases, but is still bigger than the distance between L_1 and L_2. Hence $w(\mathrm{BP}_{r,\gamma})=d(L_1,L_2)<d(\bar{L}_1,\bar{L}_2)=w(\mathrm{BP}_{r,\bar{\gamma}})$. □

We see that only if Part (a) of Lemma 4.2 holds (which is, because of $D(\mathrm{I}_\gamma)=2R(\mathrm{I}_\gamma)\cos(\gamma/2)$, equivalent to $\gamma\geqslant 2\arccos(4/3\,r)$), we have $\mathrm{I}_\gamma\subset\mathrm{BP}_{r,\gamma}$, the latter implying that $R(\mathrm{BP}_{r,\gamma})=R(\mathrm{I}_\gamma)$ and $D(\mathrm{BP}_{r,\gamma})=D(\mathrm{I}_\gamma)$.

Now considering $c+r\mathbb{B}$, we show that it is the inball of $\mathrm{BP}_{r,\gamma}$ (which means that $r(\mathrm{BP}_{r,\gamma})=r$), whenever r,γ are in the range described by the edges above. To do so, it is enough to show that L_2 does not intersect the interior of $c+r\mathbb{B}$. However, using Part (b) of Lemma 4.2, it follows that if r,γ determine a bent pentagon with maximal γ depending on r (i. e. $\mathrm{BP}_{r,\gamma}$ belongs to $(\mathbb{FR},\mathbb{SR})$ or $(\mathbb{SR},\mathbb{H})$) then L_2 does not intersect $c+r\mathbb{B}$. Decreasing γ decreases monotonously $d(L_1,L_2)$ until $\mathrm{BP}_{r,\gamma}$ becomes a set in $(\mathbb{BT},\mathbb{FR})$ or $(\mathbb{BT},\mathbb{H})$. Moreover, in both cases L_2 does not intersect $c+r\mathbb{B}$ at any point of the transformation (except that when $\mathrm{BP}_{r,\gamma}$ belongs to $(\mathbb{BT},\mathbb{H})$ it becomes tangent).

Finally, from Part (b) of Proposition 1.1, we know that the width of $\mathrm{BP}_{r,\gamma}$ must be attained between two parallel supporting lines touching the endpoints of a perpendicular segment in $\mathrm{BP}_{r,\gamma}$. However, considering the construction of the generalized bent pentagons, any such pair of parallel supporting lines, except L_1,L_2, touches an arc of $\mathrm{BP}_{r,\gamma}$ and the vertex it is drawn around. Thus the distance of any such pair of parallel supporting lines is $D(\mathrm{BP}_{r,\gamma}) \geqslant d(L_1,L_2)$ (cf. Figure 15(a)), proving $w(\mathrm{BP}_{r,\gamma}) = d(L_1,L_2)$. Observe that this argument fails if the pentagon does not fulfill Part (a) of Lemma 4.2, as p^1 would not belong to $\mathrm{BP}_{r,\gamma}$ anymore.

The given boundaries for the bent pentagons are best possible. Considering the upper bounds first, on the one hand $\gamma \leqslant \pi/3$ by definition and for all $r \in [r(\mathbb{FR}),r(\mathbb{SR})]$ this bound is reached by a maximally-sliced Reuleaux triangle $\mathrm{SR}_{r,w_r} = \mathrm{BP}_{r,\pi/3}$. On the other hand, in case of $r \in [r(\mathbb{SR}),r(\mathbb{H})]$, inequality ($ib_2$) implies that $D(\mathrm{BP}_{r,\gamma}) \geqslant r + R(\mathrm{BP}_{r,\gamma}) = D(\mathrm{BP}_{r,2\arccos((r+1)/2)})$. Taking into account that $D(\mathrm{BP}_{r,\gamma}) = D(\mathrm{I}_\gamma) = 2R(\mathrm{I}_\gamma)\cos(\gamma/2)$ as well as $D(\mathrm{I}_\gamma)$ being descending as a function of γ, the former implies that $\gamma \leqslant 2\arccos((r+1)/2)$. Equality in this situation is attained by the general hoods.

Regarding the lower bounds, in both cases choosing γ below the given bound yields a generalized bent pentagon not being a bent pentagon: As already mentioned, Part (a) of Lemma 4.2 implies $\gamma \geqslant 2\arccos(4/3r)$ in general. And in case of $r \in [r(\mathbb{BT}),r(\mathbb{H})]$ choosing $2\arccos(4/3r) \leqslant \gamma < \bar{\gamma} = \gamma_r$, Part (b) of Lemma 4.2 says that $d(L_1,L_2) < d(\bar{L}_1,\bar{L}_2)$. But since L_1 supports $c+r\mathbb{B}$ and both $\bar{L}_i, i=1,2$ support the inball of BP_{r,γ_r}, it follows that L_2 would intersect the interior of $c+r\mathbb{B}$.

For the computation of the radii we denote the angle in p^2 between $[p^1,p^2]$ and $[c,p^2]$ by α, the angle in p^2 between $[p^1,p^2]$ and L_1 by β, as well as the angle in p^2 between $[p^2,p^3]$ and the line perpendicular to L_1 by $\mu = \gamma/2 - \beta$ (cf. Figure 15(a)). Omitting again the argument $\mathrm{BP}_{r,\gamma}$ in the radii functionals, it holds

$$\text{(i)}\ \cos(\alpha) = \frac{D}{2(D-r)}, \quad \text{(ii)}\ \sin(\alpha+\beta) = \frac{r}{D-r}, \quad \text{(iii)}\ \cos(\mu) = \frac{w}{\|p^2-p^3\|}.$$

From (i) and (ii) we obtain that $\beta = \arcsin(r/D-r) - \arccos(D/2(D-r))$, which together with $\gamma = 2\arccos(D/2R)$ implies that

$$\mu = \frac{\gamma}{2} - \beta = \arccos(D/2R) + \arccos(D/2(D-r)) - \arcsin(r/D-r).$$

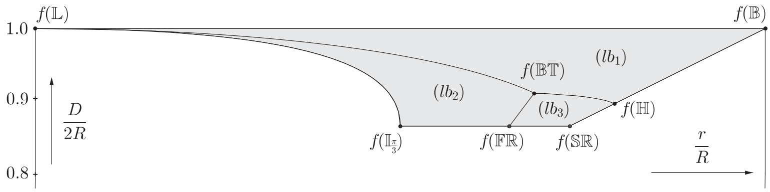

Figure 16: *Bottom view of the diagram* $f(\mathcal{K}^2)$.

Inserting μ and $\|p^2 - p^3\| = 2D\sqrt{1-(D/2R)^2}$ into (iii) results in

$$w = 2D\sqrt{1-(D/2R)^2} \cos\left(\arccos\left(\frac{D}{2(D-r)}\right) + \arccos\left(\frac{D}{2R}\right) - \arcsin\left(\frac{r}{D-r}\right)\right). \tag{6}$$

Thus each $\mathrm{BP}_{r,\gamma}$ satisfies (lb_3) with equality.

Again, we also define the bent isosceles $\mathrm{BI}_{r,\gamma} := \mathrm{conv}(\mathrm{I}_\gamma, c + r\mathbb{B})$, which obviously fulfill $R(\mathrm{BI}_{r,\gamma}) = R(\mathrm{BP}_{r,\gamma})$, $D(\mathrm{BI}_{r,\gamma}) = D(\mathrm{BP}_{r,\gamma})$, and $r(\mathrm{BI}_{r,\gamma}) = r(\mathrm{BP}_{r,\gamma})$. Using Lemma 4.2, we know that $c + r\mathbb{B}$ intersects all three edges of I_γ. However, from Part (b) of Proposition 1.1 it follows, that the width of $\mathrm{BI}_{r,\gamma}$ is necessarily attained between a parallel pair of lines, from which one supports the inball and a vertex and the other a different vertex. Doing a direct comparison among the six pairs of such parallel supporting lines, we easily obtain that $w(\mathrm{BI}_{r,\gamma}) = d(L_1, L_2) = w(\mathrm{BP}_{r,\gamma})$ (cf. Figure 15(a)). Hence it holds $f(K) = f(\mathrm{BP}_{r,\gamma})$, iff $\mathrm{BI}_{r,\gamma} \subset K \subset \mathrm{BP}_{r,\gamma}$.

(ub_2) Let $\gamma \in [\pi/3, \pi/2]$, $r \in [r(\mathrm{I}_\gamma), r(\mathrm{SB}^{\circledcirc}_\gamma)]$, and p^1, p^2, p^3 be s. t. $\mathrm{conv}\{p^1, p^2, p^3\} = \mathrm{I}_\gamma$. Then $I_K = \frac{r}{r(\mathrm{I}_\gamma)}(\mathrm{I}_\gamma - p^3) + p^3 = \mathrm{conv}\{q^1, q^2, p^3\}$ is an isosceles triangle of inradius r, s. t. $q^i = \frac{r}{r(\mathrm{I}_\gamma)} p^i + (1 - \frac{r}{r(\mathrm{I}_\gamma)}) p^3$, $i = 1, 2$ (cf. Figure 17(a)). We call the sets $\mathrm{SB}_{r,\gamma} = I_K \cap \mathbb{B}$ *(general) sailing boats*, generalizing the concentric and right-angled sailing boats which are mapped to the edges $(\mathbb{I}_{\pi/3}, \mathbb{I}_{\pi/2})$ and $(\mathbb{I}_{\pi/3}, \mathbb{SB})$.

It follows directly from the definition that $p^1 \in [q^1, p^3] \cap \mathbb{S}$ and $p^2 \in [q^2, p^3] \cap \mathbb{S}$. Hence $R(\mathrm{SB}_{r,\gamma}) = R(\mathrm{I}_\gamma)$, $D(\mathrm{SB}_{r,\gamma}) = D(\mathrm{I}_\gamma) = 2R(\mathrm{SB}_{r,\gamma}) \sin(\gamma)$ and $r(\mathrm{SB}_{r,\gamma}) = r(I_K) = r$. Moreover, since $\mathrm{I}_\gamma \subset \mathrm{SB}_{r,\gamma} \subset \mathrm{SB}^{\circledcirc}_\gamma$, the width of $\mathrm{SB}_{r,\gamma}$ is obviously taken between $[q^1, q^2]$ and p^3, s. t.

$$w(\mathrm{SB}_{r,\gamma}) = r\frac{w(\mathrm{I}_\gamma)}{r(\mathrm{I}_\gamma)} = r\left(1 + \frac{1}{\sin(\gamma/2)}\right) = r\left(1 + \frac{2\sqrt{2}R}{D}\sqrt{1 + \sqrt{1 - \left(\frac{D}{2R}\right)^2}}\right).$$

Thus all general sailing boats $\mathrm{SB}_{r,\gamma}$ are extreme for the inequality (ub_2).

Since $\mathrm{SB}_{r(\mathrm{I}_\gamma),\gamma} = \mathrm{I}_\gamma$, $\mathrm{SB}_{r(\mathrm{SB}_\gamma^{\circledcirc}),\gamma} = \mathrm{SB}_\gamma^{\circledcirc}$, and $\mathrm{SB}_{r,\pi/2}$ is a right-angled sailing-boat, the edges $(\mathbb{I}_{\pi/3}, \mathbb{I}_{\pi/2})$, $(\mathbb{I}_{\pi/3}, \mathbb{SB})$, and $(\mathbb{I}_{\pi/2}, \mathbb{SB})$ form the boundaries of this facet.

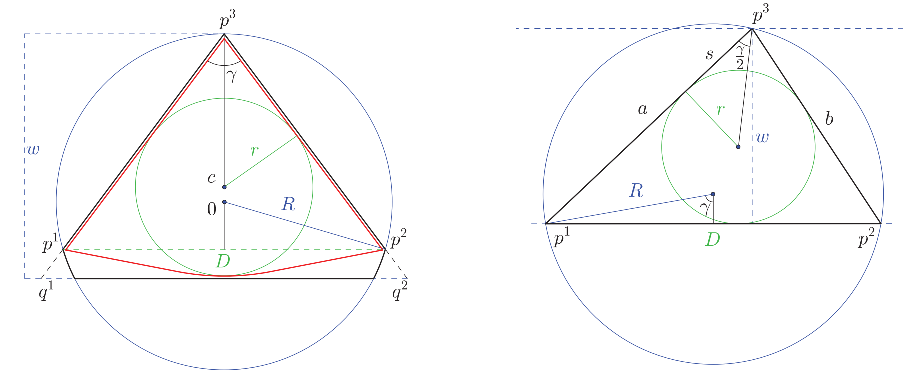

(a) *A general sailing boat* $\mathrm{SB}_{r,\gamma}$ *in black, and a corresponding minimal set in red.*

(b) *An acute triangle* $\mathrm{T}_{r,D}$.

Figure 17: *The general sailing boats and acute triangles fill the two remaining facets of the upper boundary.*

All sets K with $f(K) = f(\mathrm{SB}_{r,\gamma})$ fulfill $K \subset \mathrm{SB}_{r,\gamma}$, but in general there do not exist unique minimal sets, as we have already discussed for the edge $(\mathbb{I}_{\pi/2}, \mathrm{SB}_{r,\pi/2})$. However, if $w(\mathrm{SB}_{r,\gamma}) \leqslant \|p^1 - p^3\|$, then $\mathrm{conv}\left(\mathrm{I}_\gamma, (p^3 + w(\mathrm{SB}_{r,\gamma})\mathbb{B}) \cap \mathrm{SB}_{r,\gamma}\right)$ is a minimal unique set (cf. Figure 17(a)).

(ub_3) Any *acute triangle* is circumspherical, i. e. all its vertices are situated on the circumsphere. For any $D \in [\sqrt{3}/2, 1]$ consider the two angles $0 \leqslant \gamma_1 \leqslant \pi/3 \leqslant \gamma_2 \leqslant \pi/2$, s. t. $D(\mathrm{I}_{\gamma_1}) = D(\mathrm{I}_{\gamma_2}) = D$. It is easy to see that for any $r \in [r(\mathrm{I}_{\gamma_1}), r(\mathrm{I}_{\gamma_2})]$ there exists an acute triangle $\mathrm{T}_{r,D}$ with inradius r and the same circumradius and diameter as I_{γ_1} and I_{γ_2}.

Since every acute triangle is enclosed (in the above sense) between two isosceles triangles with the same diameter and circumradius, the edges $(\mathbb{L}, \mathbb{I}_{\pi/3})$, $(\mathbb{I}_{\pi/3}, \mathbb{I}_{\pi/2})$ (both kinds of isosceles triangles), and the edge $(\mathbb{L}, \mathbb{I}_{\pi/2})$ (right-angled triangles) form the relative boundary of this facet.

Let γ denote the angle of $\mathrm{T}_{r,D}$ at the vertex p^3, opposing the diametrical edge $[p^1, p^2]$ and s the distance within the other two edges of p^3 to the touching points of the inball with these edges (see Figure 17(b)). Then, as we have used already in the computations of the edge $(\mathbb{L}, \mathbb{I}_{\pi/2})$ in Subsection 4.2, the perimeter of $\mathrm{T}_{r,D}$ is $2(s + D)$. Thus using the semiperimeter formula for the area of a triangle, Proposition 1.3, and simple trigonometry, we have

$$\text{(i)}\ wD = 2r(s + D), \quad \text{(ii)}\ D = 2R\sin(\gamma) \quad \text{(iii)}\ r = s\tan(\gamma/2),$$

(cf. Figure 17(b)). Now, substituting the value of s in (i) by $s=\frac{r}{\tan(\gamma/2)}$ obtained from (iii), while using (ii) to replace γ, we finally arrive in

$$wD = 2r\left(D+\frac{r}{\tan\left(\frac{1}{2}\arcsin\left(\frac{D}{2R}\right)\right)}\right) = 2r\left(D+\frac{2rR}{D}\left(1+\sqrt{1-\left(\frac{D}{2R}\right)^2}\right)\right).$$

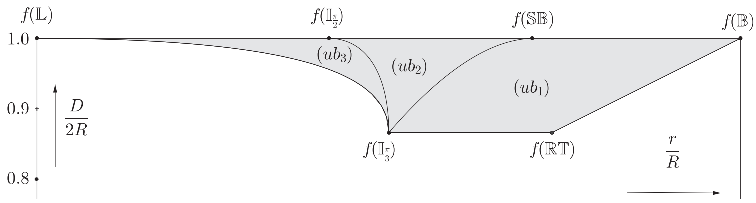

Figure 18: *Top view of the diagram* $f(\mathscr{K}^2)$.

5. Proofs of the main results

In this section we give the proofs of the main theorems. For preparation, we first state a corollary and some technical lemmas.

COROLLARY 5.1. *Let* $K\in\mathscr{K}^n$, $c\in\mathbb{R}^n$ *be,* s.t. $c+r(K)\mathbb{B}\subset K\subset\mathbb{B}$, *and let* $p^1,\dots,p^k$, $u^1,\dots,u^l$ *be as in Proposition 1.2 (a) and (b), respectively. Moreover, let* $T=c+\bigcap_{i=1}^{l}\{x\in\mathbb{R}^n : (u^i)^T x\leqslant\rho\}$ *and* $T'=\operatorname{conv}\{p^1,\dots,p^k\}$. *Then*

a) at least two of the vertices of T *do not belong to* $\operatorname{int}(\mathbb{B})$, *and*

b) T' *separates* $\operatorname{bd}(T)$ *from 0.*

Proof. Both statements follow directly from $0\in T'\subset K\subset T$, recognizing that, if all but at most one vertex of T would belong to $\operatorname{int}(\mathbb{B})$, it would follow that $R(K)\leqslant R(T)<1$, a contradiction. □

While Proposition 1.2 in Section 1 deduces properties of the inradius and the circumradius separately from their definitions, Corollary 5.1 combines them. In the following lemmas, we derive some more properties from the interaction between both parts of Proposition 1.2 and the diameter.

We recall that we always assume $\mathbb{B}$ to be the circumball of K, even though keeping the value $R(K)$ in the equations.

LEMMA 5.2. *Let* $K\in\mathscr{K}^n$ *and* $c\in\mathbb{R}^n$ *be* s.t. $c+r(K)\mathbb{B}\subset K\subset\mathbb{B}$. *Moreover let* $u^1,\dots,u^l$, T *be as in Corollary 5.1. Then there exists* $u\in\mathbb{S}$, s.t. $\mathbb{S}_u^{\geqslant}\subset T\cap\mathbb{S}$ *and* $\mathbb{S}_u^{>}\cap\operatorname{bd}(T)=\emptyset$, *iff* $K=\mathbb{B}$, $r(K)=1$ *and* $c=0$.

Proof. For the "if"-direction, we easily see that if $K = \mathbb{B}$ then choosing $l = 2$, $u^2 = -u^1$, and any u orthogonal to u^1, we obtain that $T \cap \mathbb{S} = \mathbb{S} \supset \mathbb{S}_u^{\geqslant}$ and $\mathbb{S}_u^{>} \cap \mathrm{bd}(T) = \emptyset$.

For proving the "only if"-direction let us assume $r(K) < 1$. By the definition of the points $u^1, \ldots, u^l$, we have $0 \in \mathrm{conv}\{u^1, \ldots, u^l\}$ and therefore there exists $j \in [l]$, s. t. $u^T u^j \geqslant 0$, which means $u^j \in \mathbb{S}_u^{\geqslant}$. Since $c + r(K)\mathbb{B} \subset \mathbb{B}$, it holds $\|c\| + r(K) \leqslant 1$, which means $r(K) \leqslant (u^j)^T u^j - \|c\| \left\|u^j\right\| \leqslant (u^j - c)^T u^j$ and "$=$" holds, iff $c = (1 - r(K))u^j$.

Now, in case of $(u^j - c)^T u^j > r(K)$, it follows $u^j \notin c + \{x \in \mathbb{R}^n : x^T u^j \leqslant r(K)\} \supset T \supset \mathbb{S}_u^{\geqslant}$ .On the other hand, if $(u^j - c)^T u^j = r(K)$, it holds $u^j = c + r(K)u^j \in c + \{x \in K : x^T u^j = r(K)\} \subset \mathrm{bd}(T)$. However, since $\mathbb{S}_u^{>} \cap \mathrm{bd}(T) = \emptyset$, it follows $u^j \in \mathbb{S}_u^{\geqslant} \setminus \mathbb{S}_u^{>} = \mathbb{S} \cap \{x : u^T x = 0\}$ and therefore $u^T u^j = 0$. Now, since $0 \in \mathrm{conv}\{u^1, \ldots, u^l\}$, there exists $k \in [l] \setminus \{j\}$, s. t. $u^T u^k \geqslant 0$. But, since $c + r(K)u^k \in \mathbb{S}$ would mean that there exist two different points of $c + r(K)\mathbb{B}$ in $\mathbb{S}$, contradicting $r(K) < 1$, we must have $c + r(K)u^k \notin \mathbb{S}$. Hence $(u^k - c)u^k > r(K)$ as shown above with j instead of k, contradicting $u^k \in S_u^{\geqslant}$. □

LEMMA 5.3. *Let $K \in \mathcal{K}^2$ and $c \in \mathbb{R}^2$ be* s. t. $c + r(K)\mathbb{B} \subset K \subset \mathbb{B}$, *as well as p^1, p^2, p^3 (possibly with $p^2 = p^3$), u^1, u^2, u^3 (possibly with $u^2 = u^3$), T, and T' as in Corollary 5.1 for the case $n = 2$. The common supporting lines of K and $c + r(K)\mathbb{B}$ with outer normals u^1, u^2, u^3 are denoted by L_1, L_2, L_3, respectively, the halfspaces induced by these lines containing K by L_1^-, L_2^-, L_3^- (thus $T' := \mathrm{conv}\{p^1, p^2, p^3\}$ and $T := L_1^- \cap L_2^- \cap L_3^-$). Finally, define $C := T \cap \mathbb{B}$, and $S_i := L_i \cap C$, $i = 1, 2, 3$. Then*

a) the line segments of T' separate the line segments S_i of T from 0 within $\mathbb{B}$.

b) the length of each line segment S_i, $i = 1, 2, 3$, is at most $D(K)$.

c) the diameter of C is taken between two points on different arcs of $C \cap \mathbb{S}$ or $D(C) = 2$.

d) there exist $q^1, q^2 \in C \cap \mathbb{S}$, s. t. $\left\|q^1 - q^2\right\| = D(K)$ *and the segment $[q^1, q^2]$ separates one of the segments S_i, $i = 1, 2, 3$, from the other two segments and the origin 0 (see Figure 19 as an example).*

Proof.

a) This is a direct interpretation of Part (b) of Corollary 5.1, which holds for $\mathbb{R}^2$ (but not in general).

b) If the length of S_i would be greater than $D(K)$, the same would be true for the segment of T' separating S_i from 0, a contradiction as $T' \subset K$.

c) By Proposition 1.1, there exist extreme points z^1, z^2 of C, s. t. $\left\|z^1 - z^2\right\| = D(C)$. Using Part (a) of Corollary 5.1, we distinguish the cases where no or one vertex of T belongs to $\mathrm{int}(\mathbb{B})$.

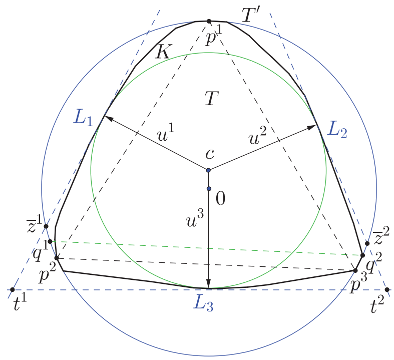

Figure 19: *A convex set* K *and all elements of Lemma* 5.3. *Observe that* $q^1 \notin K$.

In the case that no vertex of T belongs to $\mathrm{int}(\mathbb{B})$, the boundary of C alternates between the three segments L_i, $i=1,2,3$ (possibly shrinking to a single point) and three arcs in $C\cap\mathbb{S}$. Hence $z^1,z^2 \in \mathrm{ext}(C) = C\cap\mathbb{S}$. We show that if $K \neq \mathbb{B}$, then z^1 and z^2 do not belong to the same arc of $C\cap\mathbb{S}$. Let us assume that z^1 and z^2 belong to the same arc of $C\cap\mathbb{S}$ and that this arc is in between L_1 and L_2. Then we denote by $\bar{z}^i$, $i=1,2$ the one of the two endpoints of L_i, which belongs to the same arc of $C\cap\mathbb{S}$ than z^1 and z^2 (see again Figure 19). Using Lemma 5.2, we know that if $K \neq \mathbb{B}$ the arc containing z^1,z^2 is at most an open semisphere. Hence $D(C) = \left\|z^1-z^2\right\| \leqslant \left\|\bar{z}^1-\bar{z}^2\right\|$ and therefore $\{z^1,z^2\} = \{\bar{z}^1,\bar{z}^2\}$, w. l. o. g. $z^i = \bar{z}^i$, $i=1,2$. We may first assume that $L_i \cap \mathrm{int}(\mathbb{B}) \neq \emptyset$, $i=1,2$. Since $0 \in \mathrm{conv}\{u^1,u^2,u^3\}$ the lines L_i, $i=1,2$ are parallel or intersect in a vertex of T on the same side of 0 than the segment $[z^1,z^2]$. However, if the two lines are parallel or intersect, the distances between z^1 and any point in $L_2\cap\mathrm{int}(\mathbb{B})$ or the distance between z^2 and any point in $L_1\cap\mathrm{int}(\mathbb{B})$ is strictly bigger than $\left\|z^1-z^2\right\| = D(C)$, a contradiction. Now, let us assume that $L_i\cap\mathrm{int}(\mathbb{B}) = \emptyset$ for at least one $i \in \{1,2\}$, w. l. o. g. for $i=1$. This means $\{z^1\} = L_1\cap\mathbb{S}$ and therefore L_1 supports $\mathbb{B}$ in z^1. By definition L_1 supports $c+r(K)\mathbb{B}$. Hence we obtain that L_1 support $c+r(K)\mathbb{B}$ in z^1. Using the fact that the arc containing z^1,z^2 is at most an open semisphere, we have $z^2 \neq -z^1$ and therefore $D(C) \geqslant D(\mathrm{conv}(\{z^2\}\cup(c+r(K)\mathbb{B})) > \left\|z^1-z^2\right\| = D(C)$, again a contradiction.

Finally, consider the case that one vertex of T belongs to $\mathrm{int}(\mathbb{B})$. Then C possesses only two arcs in $C\cap\mathbb{S}$ (possibly be split by a single pointed L_i). Applying Part (a) of Proposition 1.2 for C, there exist p^1,p^2,p^3 in this two arcs, s. t. $0 \in \mathrm{conv}\{p^1,p^2,p^3\}$. However, as two of the p^i have to be on the same arc, the negative of the third has to be on that arc, too, proving $D(C)=2$ for that case.

d) In case of $K=\mathbb{B}$ the claim is trivially true. Hence we may assume $K\neq\mathbb{B}$.

Using Part (a) of Corollary 5.1, we distinguish again the cases with no or one vertex of T belonging to $\mathrm{int}(\mathbb{B})$.

In the first case, it was shown in Part (c) that any pair of diametrical points z^1 and z^2 of C lie in different arcs of $C \cap \mathbb{S}$. This means that $[z^1, z^2]$ separates one of the segments S_i from the other two segments and the origin 0, say S_3 (cf. Figure 19). From Part (b) we know that the length of S_3 is at most $D(K) \leqslant D(C) = \|z^1 - z^2\|$. Hence there exist q^1 and q^2 in the same arcs as z^1 and z^2, respectively, s.t. $\|q^1 - q^2\| = D(K)$ and $[q^1, q^2]$ still separates S_3 in the same way as $[z^1, z^2]$ does.

In case that one vertex of T belongs to $\operatorname{int}(\mathbb{B})$, it follows from Part (c) that $D(C) = 2$, which means $z^2 = -z^1$. Thus $[z^1, z^2]$ separates the two segments intersecting in $\operatorname{int}(\mathbb{B})$ from the third. Again because of Part (b) there must exist q^1 and q^2 with $\|q^1 - q^2\| = D(K)$ separating this third segment from the other two and 0. □

LEMMA 5.4. *Consider the same setting and notation as in Lemma 5.3. In the following we assume that the single separated segment in Part (d) of Lemma 5.3 is S_3 and* w.l.o.g. *that S_3 is horizontal below 0 as well as separated by $[q^1, q^2]$ from S_1, S_2, and 0. Moreover, we denote the point in C farthest from L_3 by y, the intersection points of L_i, $i = 1, 2$ with L_3 by t^i, $i = 1, 2$, respectively, and assume that $t^1_1 \leqslant 0 \leqslant t^2_1$ (which is possible when S_3 is horizontal and means that L_1 bounds S_3 on the left while L_2 bounds S_3 on the right, see Figure 19).*

a) *The first coordinate of the intersection points of L_1 and $\mathbb{S}$ is bounded from above by $D(K)/2$ while the first coordinate of the intersection points of L_2 and $\mathbb{S}$ is bounded from below by $-D(K)/2$.*

b) *It holds $|y_1| \leqslant D(K)/2$.*

c) *One can modify the choice of q^1 and q^2 satisfying Part (d) in Lemma 5.3,* s.t. *the interior angles of* $\operatorname{conv}\{y, q^1, q^2\}$ *in q^1 and q^2 are at most $\pi/2$.*

Proof.

a) It suffices to show the upper bound in case of L_1. Since S_3 is the separated segment, it follows that $t^1, t^2 \notin \operatorname{int}(\mathbb{B})$ and since S_3 is horizontal, (a) is obviously true for $\bar{z}^1$. Let us denote the other endpoint of S_1 by x^1 and assume $x^1_1 \geqslant 0$ as otherwise there is nothing to show. Since S_3 is horizontal and lower bounding C, we have $t^1_2 \leqslant x^1_2$. Together with $t^1_1 \leqslant 0$ this means L_1 has a positive slope. Moreover, to keep 0 within C it must hold that $-\bar{z}^1_1 \geqslant x^1_1$. Now, assuming $x^1_1 > D(K)/2$ would also imply $\bar{z}^1_1 < -D(K)/2$ and therefore that the length of S_1 would be strictly greater than $D(K)$, which contradicts Part (b) of Lemma 5.3.

b) Again, it suffices to show $y_1 \leqslant D(K)/2$, because of symmetry in the argument. If L_1 and L_2 intersect within $\operatorname{int}(\mathbb{B})$, they must intersect in y. Hence $y_1 \leqslant x^1_1 \leqslant D(K)/2$ using the notation as in Part (a). Otherwise y lies on the arc of $C \cap \mathbb{S}$ bounded by x^1 and the upper intersection point x^2 of L_2 and $\mathbb{S}$. However, with e^2 denoting the second unit vector, that would mean $y \in \{x^1, x^2, e^2\}$, which again proves the claim because of Part (a).

c) We suppose w. l. o. g. that q^i, $i=1,2$, belong to the arc of $\mathbb{S}$ induced by S_i and S_3, $i=1,2$, respectively. Now, assuming that one of the interior angles of $\operatorname{conv}\{y,q^1,q^2\}$ in q^1 or q^2 is bigger than $\pi/2$ would mean that y lies in one of the two open caps of $\mathbb{B}$ separated from 0, obtained from cutting $\mathbb{B}$ with $\operatorname{aff}\{q^1,-q^2\}$ or $\operatorname{aff}\{-q^1,q^2\}$. Denoting the intersection point of L_1 and L_2 by t^3, we know from Part (b) that $y\in\{x^1,x^2,e^2,t^3\}$. In any of the four cases $[q^1,q^2]$ separates y from S_3.

Now, we describe the choice of q^1 and q^2 satisfying the statement for each of the four possible y's: Since $q^1_1<0$ and $q^2_1>0$, e^2 can obviously not belong to one of the two open caps described above. To obtain that $y=x^i$, $i=1,2$, it must hold that e^2 does not belong to C. In that case either $x^1_1>0$ and $y=x^1$ or $x^1_2<0$ and $y=x^2$. We may assume w. l. o. g. that $y=x^1$ or $y=t^3$ and that, if y belongs to one of the open caps, then it is contained in the cap induced by $\operatorname{aff}\{-q^1,q^2\}$. Using Part (b) of Lemma 5.3, we know that the length of S_1 is at most $D(K)=\|q^1-q^2\|$. However, since y is contained in the open cap of $\mathbb{B}$ induced by $\operatorname{aff}\{-q^1,q^2\}$, the length of S_1 can only be bounded by $D(K)$ if S_1 cuts through one of the segments $[q^1,q^2]$ or $[-q^2,-q^1]$. However, the first case would contradict that $[q^1,q^2]$ separates S_1 from S_3. Hence S_1 must intersect $[-q^2,-q^1]$. Now, S_3 is horizontal and therfore S_1 ascending (and S_2 descending). Moreover, since y is in the open cap induced by $\operatorname{aff}\{-q^1,q^2\}$ we have $-q^1$ possesses a bigger second coordinate than y. Thus the segment $[q^1,q^2]$ must be ascending, even with a bigger slope than S_1, since otherwise S_1 and $[-q^2,-q^1]$ could not intersect. But if this is the case, we may move $q^1,q^2\in C\cap\mathbb{S}$, within the arcs they belong to, keeping their distance, until $[q^1,q^2]$ becomes parallel to S_1. Since this means $[q^1,q^2]$ stays ascending with the new points q^1 and q^2, it still separates S_3 from S_1, S_2 and 0. Moreover, the open caps now induced by $\operatorname{aff}\{q^1,-q^2\}$ and $\operatorname{aff}\{-q^1,q^2\}$ do not contain y anymore, implying that the interior angles of $\operatorname{conv}\{y,q^1,q^2\}$ in q^1 and q^2 are at most $\pi/2$ now. □

Before considering the next Lemma, remember that we know from the facets (ub_2) and (ub_3) in Subsection 4.3, that for every diameter $D\in[\sqrt{3},2]$ and inradius $r\in[r(\mathrm{I}_{2\arccos(D/2)}),r(\mathrm{SB}^{\circledcirc}_{\arcsin(D/2)})]$ there exist triangles $\mathrm{T}_{r,D}$ (in case of $r\leqslant r(\mathrm{I}_{\arcsin(D/2)})$) or sailing boats $\mathrm{SB}_{r,\arcsin(D/2)}$ (in case of $r\geqslant r(\mathrm{I}_{\arcsin(D/2)})$).

LEMMA 5.5. *Let* $D\in[\sqrt{3},2]$ *and* $r(\mathrm{I}_{2\arccos(D/2)})\leqslant r\leqslant r(\mathrm{SB}^{\circledcirc}_{\arcsin(D/2)})$. *Then for all* $K\in\mathscr{K}^2$, s. t. $D(K)=D$ *and* $r(K)=r$ *there exists*

a) a triangle $\mathrm{T}_{r,D}$, s. t. $w(K)\leqslant w(\mathrm{T}_{r,D})$, *if* $r\leqslant r(\mathrm{I}_{\arcsin(D/2)})$, *and*

b) a sailing boat $\mathrm{SB}_{r,\arcsin(D/2)}$, s. t. $w(K)\leqslant w(\mathrm{SB}_{r,\arcsin(D/2)})$, *if* $r\geqslant r(\mathrm{I}_{\arcsin(D/2)})$.

Proof. Let $c\in\mathbb{R}^2$ be s. t. $c+r(K)\mathbb{B}$ and $\mathbb{B}$ are the in- and circumball of K, respectively. Using the notation as given in Lemma 5.3, remember that $R(C)=R(K)$ and $r(C)=r(K)$, whereas the monotonicity of the radii with respect to set inclusion implies $D(C)\geqslant D(K)$ and $w(C)\geqslant w(K)$.

The idea of the present proof is to transform C in several steps into some triangle or sailing boat $\bar{C}$ satisfying $R(\bar{C}) = R(K)$, $r(\bar{C}) = r(K)$, $D(\bar{C}) = D(K)$, and $w(\bar{C}) \geqslant w(K)$.

More precisely, denoting the breadth of C in direction of u^3 by $b_{u^3}(C)$, we know from the definitions of the width that $w(C) \leqslant b_{u^3}(C) = \mathrm{dist}(y, L_3)$ as the point y in Lemma 5.4 is the farthest point from L_3 in C.

Now, in every step of the transformation of C, we will increase the breadth in direction of u^3, but, when arriving in $\bar{C}$, it even holds $w(\bar{C}) = b_{u^3}(\bar{C})$ (as we have seen when defining the triangle and sailing boat families).

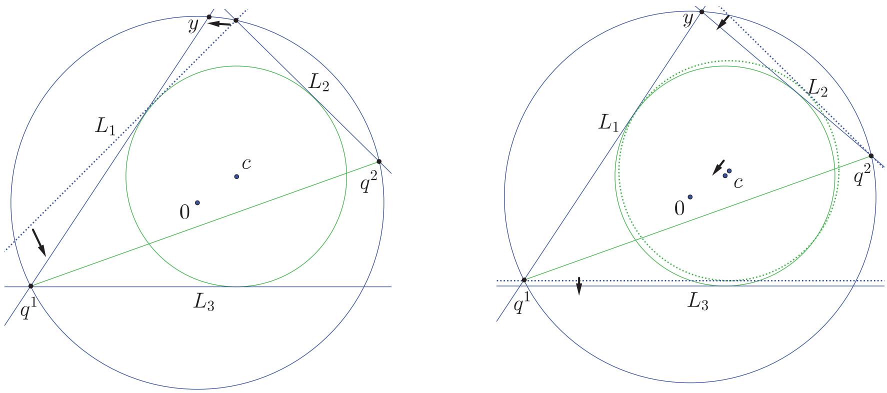

(a) *In (i) the lines* L_1, L_2 *may be rotated around* $c + r\mathbb{B}$.

(b) *In (ii) we may move* $c + r\mathbb{B}$ *downwards while* L_1 *(and/or* L_2 *) may be rotated around* q^1 *(and/or* q^2 *).*

Figure 20: *Examples for (i) and (ii) in Lemma 5.5. Here and in Figures 21 to 23 the start and the end of a movement are indicated by dotted and, respectively, full lines.*

(i) Rotate the lines L_1 and L_2, s. t. they keep supporting $c + r(K)\mathbb{B}$ and contain q^1 and q^2, respectively, thus also keeping the separation of S_1, S_2 from S_3 by $[q^1, q^2]$. In the degenerate case of only two supporting parallel lines to $c + r(K)\mathbb{B}$ (which means by the choices in the proof of Lemma 5.3 that $u^1 = u^2$), we substitute L_1 by two lines L_1 and L_2 supporting $c + r(K)\mathbb{B}$ and containing q^1 and q^2, respectively, s. t. $0 \in \mathrm{int}(\mathrm{conv}\{u^1, u^2, u^3\})$ and arrive in the same situation than in the non-degenerate case.

   Thus, the y we have before the change still belongs to C afterwards and therefore the new y (the point at maximum distance from L_3 within the new C) is not closer to L_3 than before. Applying Parts (b) and (c) of Lemma 5.4 for the new C, we still have that $|y_1| \leqslant D(K)/2$ and that $\mathrm{conv}\{y, q^1, q^2\}$ has interior angles in q^1 and q^2 at most $\pi/2$.

(ii) This step is only needed, if $L_1 \cap L_2 \notin \mathbb{B}$, which means that $y \in \{x^1, x^2, e^2\}$. First, as long as $y \notin L_2$ we translate $c + r(K)\mathbb{B}$ downwards, parallel to L_1, rotate L_2 around the point q^2 and move L_3 parallel to its prior position, s. t. L_2 and L_3 keep supporting $c+r(K)\mathbb{B}$. Afterwards, as long as $y \notin L_1$ we translate $c+r(K)\mathbb{B}$ downwards, parallel to L_2, rotate L_1 around the point q^1, and move L_3 again parallel to its prior position, s. t. L_1 and L_3 keep supporting $c+r(K)\mathbb{B}$. In the end y is in $L_1 \cap L_2 \cap \mathbb{S}$ and since L_3 moves always vertically downwards, but y stays equal, the distance $\mathrm{dist}(\mathrm{y}, \mathrm{L}_3)$ does not decrease.

(iii) Since the inner angles of $\mathrm{conv}\{y, q^1, q^2\}$ in q^1 and q^2 are at most $\pi/2$, it holds $\|t^1 - t^2\| \geqslant \|q^1 - q^2\| = D(K)$, recalling that t^i denotes the intersection point of L_3 with L_i, $i = 1,2$. Hence there exist $\bar{q}^i \in L_i$, $i = 1,2$, s. t. $[\bar{q}^1, \bar{q}^2]$ is parallel to L_3 and $\left\|\bar{q}^1 - \bar{q}^2\right\| = D(K)$. Now, we translate T until $\bar{q}^i$, $i = 1,2$ become the points $\left(\pm D/2, -\sqrt{1-(D/2)^2}\right)^T \in \mathbb{S}$ (see Figure 21(a)).

From (ii) it follows $y \in L_1 \cap L_2 \subset \mathbb{B}$ and since T is only translated in (iii) neither the $\mathrm{dist}(\mathrm{y}, \mathrm{L}_3)$ nor the angle in y of T changes. Since we also have $\left\|\bar{q}^1 - \bar{q}^2\right\| = \|q^1 - q^2\|$ Proposition 1.3 (with y in the role of p^3 there) implies that after the movement the vertex y is still in $\mathbb{B}$, and moreover, if $y \in \mathbb{S}$ before the movement, it will be in $\mathbb{S}$ after, too.

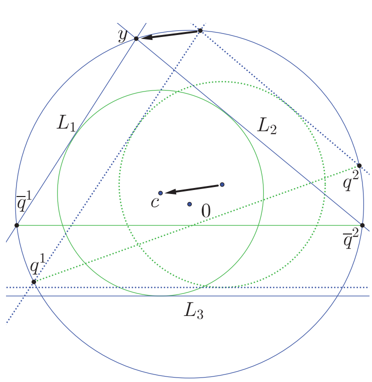

(a) *In (iii) the set rotates until $[q^1, q^2]$ becomes parallel to L_3.*

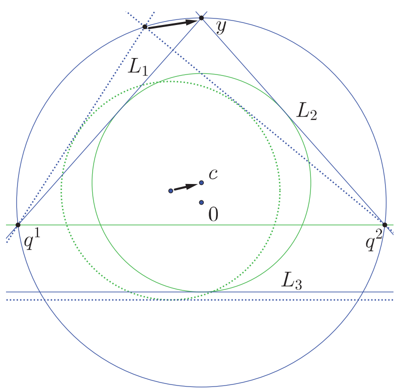

(b) *In (iv) (if $y \in \mathbb{S}$) y moves inside $\mathbb{S}$ and may become e^2 whereas $C = \mathrm{SB}_{r,\gamma}$.*

Figure 21: *Examples of (iii) and (iv) from Lemma 5.5.*

(iv) If $y \in \mathbb{S}$, we move $\{y\} = L_1 \cap L_2$ around $\mathbb{S}$ towards e^2 and L_1 and L_2 with it. The inball is moved, s. t. it remains tangent to both L_1 and L_2 and the line L_3 parallel to its prior position to keep tangent to the inball. We stop when $y = e^2$ (see Figure 21(b)) or L_3 contains the segment $[q^1, q^2]$ (whichever comes first –

the first stopping reason meaning that C becomes a sailing boat, the latter that C becomes a triangle).

Before and after the transformation the inradius and the angles in the points y of the two triangles coincide (see Proposition 1.3), while the line passing through the incenter c and y becomes closer to be perpendicular to L_3. Hence the distance $\mathrm{dist(y,L_3)}$ does not decrease under this movement.

If $y = e^2$, then $C = \mathrm{SB}_{r(K),\gamma(D(K))}$, otherwise, if L_3 contains the segment $[q^1,q^2]$, $C = \mathrm{T}_{r(K),D(K)}$. In both cases $r(C) = r(K), D(C) = D(K)$, $R(C) = R(K)$, and $w(C) = \mathrm{dist(y,L_3)} \geqslant b_{u^3}(K) \geqslant w(K)$ holds.

(v) If $y \in \mathrm{int}(\mathbb{B})$, we rotate the lines L_1, L_2 around q^1, q^2, repectively, s. t. $\{y\} = L_1 \cap L_2$ moves along $\mathrm{aff}\{y,c\}$ away from c. The inball moves, s. t. it remains tangent to L_1 and L_2, while L_3 is shifted upwards, parallel to its original position to remain tangent to the inball.

The transformation finishes when $y \in \mathbb{S}$ or the line L_3 contains the segment $[q^1,q^2]$.

Before and after the movement the triangle T has the same inradius and $\mathrm{aff}\{y,c\}$ has the same angle with respect to L_3, but the angle in y decreases. Hence the distance $\mathrm{dist(y,L_3)}$ does not decrease.

If we arrive in $y \in \mathbb{S}$, we are in a situation to apply (iv) again. If L_3 contains the segment $[q^1,q^2]$, then we may roll the inball along L_3 and rotate L_i, $i = 1,2$, s. t. they keep supporting the inball, until $y \in \mathbb{S}$. Hence the inball of $\mathrm{conv}\{y,q^1,q^2\}$ stays equal and it can easily be checked that the width of the triangle does not decrease under this transformation. In fact, we again arrive in the situation $C = \mathrm{T}_{r(K),D(K)}$ as after (iv), when $y \neq e^2$. □

Proof of Theorem 3.4. The part of Theorem 3.4 that all sailing boats fulfill equality for (ub_2) directly follows from the description of sailing boats in Subsection 4.3. Thus it only remains to show the general validity of the inequality (ub_2).

Since there exist isosceles triangles I_γ and concentric sailing boats $\mathrm{SB}^{\circledcirc}_\gamma$ of the same diameter and circumradius as a given K for an appropriate choice of $\gamma \in [\pi/3, \pi/2]$, we only have to distinguish the cases

$$\text{(i)}\quad r(K) \leqslant r(\mathrm{I}_\gamma), \qquad \text{(ii)}\quad r(\mathrm{I}_\gamma) \leqslant r(K) \leqslant r(\mathrm{SB}^{\circledcirc}_\gamma), \qquad \text{(iii)}\quad r(K) \geqslant r(\mathrm{SB}^{\circledcirc}_\gamma).$$

Again we abbreviate $r = r(K), w = w(K), D = D(K)$, and $R = R(K) = 1$.

In case of (ii), K fulfills the conditions of Part (b) in Lemma 5.5 and we obtain that $w \leqslant w(\mathrm{SB}_{r,D})$, which suffices as mentioned above. For the other two cases we *extend* the construction of the general sailing boats from Subsection 4.3:

For any pair r,D obtained from K, let $\mathrm{I}_\gamma = \mathrm{conv}\{p^1,p^2,p^3\}$, $\gamma \in [\pi/3, \pi/2]$ be the isosceles triangle with circumball $\mathbb{B}$ and diameter $D = \left\|p^1 - p^2\right\|$ as well as $I_K := r/r(\mathrm{I}_\gamma)(\mathrm{I}_\gamma - p^3) + p^3$ the rescaled copy with inradius r, keeping the vertex p^3.

By construction, I_K belongs to the general sailing boats, $D(I_K) = {}^{r}/_{r(\mathrm{I}_\gamma)} D$, and $R(I_K) = {}^{r}/_{r(\mathrm{I}_\gamma)} R$. Hence it fulfills ($ub_2$) with equality. However, since

$$r(I_K)\left(1+\frac{2\sqrt{2}R(I_K)}{D(I_K)}\sqrt{1+\sqrt{1-\left(\frac{D(I_K)}{2R(I_K)}\right)^2}}\right)$$
$$= r\left(1+\frac{2\sqrt{2}R}{D}\sqrt{1+\sqrt{1-\left(\frac{D}{2R}\right)^2}}\right)$$

it suffices to show that $w \leqslant w(I_K)$.

Now, we first consider Case (i): using Lemma 5.5 and the notation used there, we know there exists a triangle $\mathrm{T}_{r,D} = \mathrm{conv}\{q^1, q^2, y\}$, s. t. $\|q^1 - q^2\| = D$ and $w \leqslant w(\mathrm{T}_{r,D}) = \mathrm{dist}(\mathrm{y}, [\mathrm{q}^1, \mathrm{q}^2])$. Hence we just need to prove $w(\mathrm{T}_{r,D}) \leqslant w(I_K)$.

Similar to (iv) of Lemma 5.5, we now transform $\mathrm{T}_{r,D}$ by moving y within $\mathbb{S}$ until $y = p^3$, ignoring the stopping condition "when L_3 contains $[q^1, q^2]$". Because of ignoring the stopping condition, the inball will not touch $[q^1, q^2]$ anymore, but a line L parallel to $[q^1, q^2]$, which means that we obtained at a triangle congruente with I_γ and inradius r, which is I_K. Thus $\mathrm{dist}(\mathrm{p}^3, \mathrm{L}) = w(I_K)$ and we may argue as in (iv) of Lemma 5.5 that $w(\mathrm{T}_{r,D}) \leqslant w(I_K)$, which shows the assertion.

Finally, assume we are in case of (iii). We know from Subsection 4.3 that the outer parallel bodies K' of a concentric saling boat or a Reuleaux blossom satisfy $r(K') = r$, $D(K') = D$, $R(K') = R$, and $w \leqslant w(K') = r(K') + R(K')$. Hence we just need to show that $w(K') \leqslant w(I_K)$ again.

Now, consider the concentric sailing boat $\mathrm{SB}_\gamma^{\circledcirc}$. It shares p^3 and its inside angle γ with I_K and has a smaller inradius. Thus it follows from the concentricity of the in- and circumradius of $\mathrm{SB}_\gamma^{\circledcirc}$ that $c_2 < 0$ holds for the incenter c of I_K. Hence $w(I_K) = r + R + |c_2| \geqslant r(K') + R(K') = w(K')$ which finishes the proof. □

Proof of Theorem 3.5. In case of $r(K) \leqslant r(\mathrm{I}_{\arcsin(D(K)/2R(K))})$ Part (a) of Lemma 5.5 implies $w(K) \leqslant w(\mathrm{T}_{r,D})$, proving the validity of (ub_3) in that case.

Thus we may assume w. l. o. g. that $r(K) \geqslant r(\mathrm{I}_{\arcsin(D(K)/2R(K))})$. Observe two facts: first, if $r(K) = r(\mathrm{I}_{\arcsin(D(K)/2R(K))})$, then the two right hand sides of (ub_2) and (ub_3) coincide and equal $w(\mathrm{I}_{\arcsin(D(K)/2R(K))})$. Omitting again the argument K, we obtain that

$$\frac{w}{r} = 1+\frac{2\sqrt{2}R}{D}\sqrt{1+\sqrt{1-\left(\frac{D}{2R}\right)^2}} = \frac{2}{D}\left(D+\frac{2rR}{D}\left(1+\sqrt{1-\left(\frac{D}{2R}\right)^2}\right)\right) \tag{7}$$

in that case. The second fact to be observed is that in (7) the middle expression does not depend on r, while the right hand part is increasing in r. Hence knowing the general validity of (ub_2), we may conclude

$$\frac{w}{r} \leqslant 1+\frac{2\sqrt{2}R}{D}\sqrt{1+\sqrt{1-\left(\frac{D}{2R}\right)^2}} \leqslant \frac{2}{D}\left(D+\frac{2rR}{D}\left(1+\sqrt{1-\left(\frac{D}{2R}\right)^2}\right)\right). \qquad \square$$

Now, we turn to the open part of the lower boundary and start with a technical corollary needed in order to prove Theorem 3.2.

COROLLARY 5.6. *Let $K \in \mathscr{K}^n$ and $c \in \mathbb{R}^n$ be* s. t. $c + r(K)\mathbb{B}$ *and* $\mathbb{B}$ *are the in- and circumball of* K*, respectively. Moreover, let* $p^1, \dots, p^k \in K \cap \mathbb{S}$ *be the points given by Part (a) of Proposition* 1.2*,* $T' := \mathrm{conv}\{p^1, \dots, p^k\}$*, and* $C := \mathrm{conv}(T', c + r(K)\mathbb{B})$*. Then* $D(C) = \max\{D(T'), \|p^i - c\| + r(C), i \in [k]\}$*.*

Proof. Since the statement is obviously true if $K = \mathbb{B}$, we may assume w. l. o. g. that $K \neq \mathbb{B}$ and therefore $C \neq \mathbb{B}$. This means the diameter of C is bigger than $2r(C)$, the distance of two antipodal points of the inball. However, due to Proposition 1.1 the diameter is attained between two extreme points. Thus if it is not attained between a pair of the vertices $p^1, \dots, p^k$, it must be between one of them and its antipodal on the insphere. □

REMARK 5.7. Let $K \in \mathscr{K}^2$, $c \in \mathbb{R}^2$, $p^1, \dots, p^k \in K \cap \mathbb{S}$, T', and C be given as in Corollary 5.6. Denoting by L_1, L_2 a pair of parallel supporting lines of C, s. t. $w(C) = d(L_1, L_2)$ we may assume w. l. o. g. due to Proposition 1.1 that L_1 has at least two contact points with C and (by renaming and defining $p^3 = p^2$ if necessary) that p^1 is situated in one of the arcs in $\mathbb{S}$ between L_1 and L_2, while p^2 and p^3 belong to the other with p^2 closer to L_1 and p^3 closer to L_2. With this assumptions one of the following cases holds:

(i) L_1 contains p^2 but not p^1 and supports $c + r(K)\mathbb{B}$, whereas L_2 supports $c + r(K)\mathbb{B}$.

(ii) L_1 contains p^2 but not p^1 and supports $c + r(K)\mathbb{B}$, whereas L_2 contains only p^3.

(iii) L_1 contains p^1 but not p^2 and supports $c + r(K)\mathbb{B}$, whereas L_2 contains only p^3.

(iv) L_1 contains $[p^1, p^2]$, whereas L_2 contains p^3 or supports $c + r(K)\mathbb{B}$.

Due to Proposition 1.1 one of the sets $L_i \cap C$, $i = 1, 2$, say $L_1 \cap C$ contains a smooth boundary point of C. Hence $L_1 \cap C$ is either a segment containing at least one of the points p^1, p^2, which means we are in Case (ii),(iii), or (iv), or L_1 supports the inball in a unique point (see Figure 22(a) for an example of Case (ii)). However, in case $L_2 \cap C$ is a segment, we may interchange the roles of L_1 and L_2 arriving again in Case (ii), (iii), or (iv), or in the case that L_2 also supports C only in a single boundary point of the inball. In case of the latter situation we may rotate L_1 and L_2 around the inball, s. t. we may assume Case (i).

The following lemma proves Theorem 3.2 apart from the general validity of the inequality.

LEMMA 5.8. *Let $K \in \mathscr{K}^2$ be* s. t. *there exists a bent pentagon* $\mathrm{BP}_{r,\gamma}$ *from the facet* (lb_3) *with the same inradius, circumradius and diameter as* K*. Then* $w(K) \geqslant w(\mathrm{BP}_{r,\gamma})$*.*

Proof. Using the same notation as in Corollary 5.6 we have $r(C) = r(K)$ and $R(C) = R(K)$ by definition as well as $D(C) \leqslant D(K)$ and $w(C) \leqslant w(K)$ because of the monotonicity of the radii with respect to set inclusion.

The idea of the proof is to transform C in several steps into a bent isosceles $\mathrm{BI}_{r,\gamma}$ from (lb_3) of Subsection 4.3 keeping the same in- and circumradius at all time and guaranteeing that $D(\mathrm{BI}_{r,\gamma}) = D(K)$ and $w(\mathrm{BI}_{r,\gamma}) \leqslant w(K)$ at the end of the transformation (and obtaining the corresponding solution for $\mathrm{BP}_{r,\gamma}$). More precisely, we know that the parallel supporting lines L_1 and L_2 of C from Remark 5.7 satisfy $w(C) = d(L_1, L_2)$. Now, $d(L_1, L_2)$ will be decreased in every step of the transformation of C, but when arriving at $\mathrm{BI}_{r,\gamma}$ it again holds $w(\mathrm{BI}_{r,\gamma}) = d(L_1, L_2)$ (as shown in (lb_3)).

To reduce notation formalities we assume w. l. o. g. that L_1, L_2 are embedded horizontally and we denote the inball by $c + r\mathbb{B}$.

(a) The first step is only needed in case of $c_1 < 0$. In this step all radii except the diameter of C are kept constant, while the diameter may be reduced but not raised.

If L_1 and L_2 are arranged as in Case (iii) of Remark 5.7, then using Part (b) of Proposition 1.1, we see that $c_1 < 0$ is not possible as $c_1 \geqslant p_1^3 \geqslant 0$ holds. In case of Case (ii) or Case (iv), we may translate $c + r\mathbb{B}$ parallel to L_1 until $c_1 = 0$. Because of Corollary 5.6 this transformation does not increase $D(C)$: in both cases the only candidate distance for the diameter which is raised is $\|p^1 - c\| + r(C)$, but in case of (iv) $\|p^1 - c\|$ is before and after the transformation bounded from above by $\|p^2 - c\|$ and in case of (ii) it is bounded from above by $\|p^2 - c\|$ or by $\|p^3 - c\|$.

Finally, Case (i) can be handled almost the same. If p^3 is closer to L_2 than p^1, again $\|p^2 - c\|$ is bounded from above by $\|p^2 - c\|$ or by $\|p^3 - c\|$ and we may directly move $c + r\mathbb{B}$ parallel to L_1 until $c_1 = 0$. If, on the contrary, p^1 is the point closer to L_2, then we first rotate C between L_1 and L_2 until p^1 and p^3 get equidistant with respect to L_2 and then we may do the movement of $c + r\mathbb{B}$.

(b) Translate p^2 and p^3 on $\mathbb{S}$ within the arcs between L_1 and L_2 they belong to, until $\|p^1 - p^2\| = \|p^1 - p^3\| = D(K)$. Since $c_1 \geqslant 0$ and $D(C) \leqslant D(K)$ before the transformation, we have $D(C) = D(K)$ after the transformation and we keep at least p^1 on L_1 or L_1 tangent to the unit ball. Moreover, if necessary, moving L_2 parallel to its prior position until it supports C again, L_2 touches p^3 or $c + r\mathbb{B}$ (see Figure 22(a)), $d(L_1, L_2)$ does not increase, and $r(C)$ and $R(C)$ stay constant.

However, in each situation where we only touch two points after the transformation, we may additionally rotate L_1 and L_2 around the vertices or along the insphere, respectively, not increasing their distance, until we obtain a third touching point of the two lines with C. In the following we distinguish the following cases, (exchanging, if necessary, the roles of L_1, L_2 and p^2, p^3, respectively, to attain one of them):

(i) L_1 contains p^1, or

(ii) L_1 contains p^2 and supports $c + r\mathbb{B}$ and L_2 contains p^3, or

(iii) L_1 does not contain any of the points p^i, while L_2 contains p^3 but no other.

In all three cases we will search for a situation, in which the angle between L_1 with one of the edges of I_γ is acute. If (i) holds, the angle between L_1 and $[p^1, p^3]$ must always be acute as p^3 lies on the right side of p^1.

In case of (ii), the angle between L_1 and $[p^2, p^3]$ can either be acute (see Figure 22(b)) or obtuse, as p^3 could even be on the right of p^2. If the latter happens we rotate L_1 around p^2 (thus possibly loosing contact with $c + r\mathbb{B}$) and L_2 around p_3, keeping them parallel. This is done until L_2 supports $c + r\mathbb{B}$, allowing a zero degree rotation in the case that L_2 supported $c + r\mathbb{B}$ from the beginning. This does not increase $d(L_1, L_2)$.

Finally if (iii) holds, the angle between L_2 and $[p^2, p^3]$ could be obtuse. Then we rotate both lines L_1, L_2 along $c + r\mathbb{B}$, loosing contact with p^3, until L_2 touches p^1 or L_1 touches p^2 (whichever comes first). In case L_2 touches p^1 first we are back in (i). Thus assume L_1 touches p^2 first and compare $\mathrm{conv}\{p^1, p^2, p^3, c + r\mathbb{B}\}$ with the bent isosceles $\mathrm{BI}_{r,\gamma}$ we want to arrive at: Because of our movement in the beginning of (b), we have that $\mathrm{conv}\{p^1, p^2, p^3\}$ is an isosceles triangle with inball $c + r\mathbb{B}$ contained in C. Hence identifying it with $\mathrm{I}_\gamma \subset \mathrm{BI}_{r,\gamma}$ yields that the supporting lines L_1', L_2' of $\mathrm{BI}_{r,\gamma}$ contain p^2 and p^3, respectively, and contain between them the inball of radius r. Thus it holds $\|p^2 - p^3\| \geqslant 2r$. Considering C again, since the angle between L_2 and $[p^2, p^3]$ was obtuse before the rotation of L_1, L_2 in (iii), the incenter c is closer to p^3 than to p^2. But since $\|p^2 - p^3\| \geqslant 2r$, this means

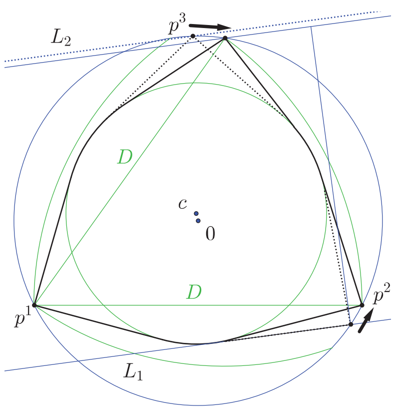

(a) *In (b), the tangencies correspond to Part (ii) of Remark 5.7. While moving p^2, p^3, L_1 and L_2 some of the tangencies can be lost but we obtain that I_γ is contained in C.*

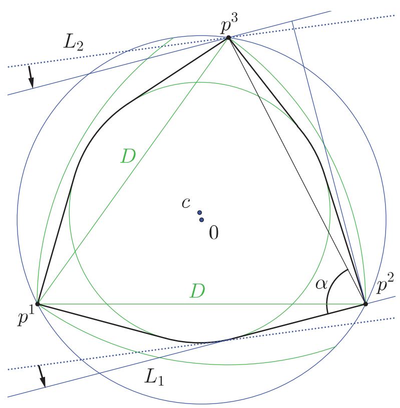

(b) *We rotate L_1, L_2 around C until L_1 or L_2 supports more than one point of C, arriving, e. g., in the situation in which L_1 contains p^2 and supports $c + r\mathbb{B}$, L_2 supports p^3, and α is acute here. Then we are back into the tangencies of Part (ii).*

Figure 22: *Transformations of C during (b). Here the green bows indicate arcs of radius D and centers in p^1, p^2, p^3, defining a region in which both, $c + r\mathbb{B}$ and the p^i, have to be contained.*

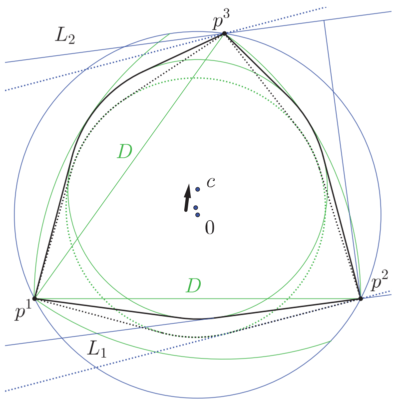

Figure 23: *In (c) the inball moves, L_1 is rotated around p^2 reducing the angle with $[p^2,p^3]$ and L_2 to keep parallel with L_1 until $C = \mathrm{BI}_{r,\gamma}$.*

after the rotation the angle between L_1 and $[p^2,p^3]$ must be acute. Exchanging if necessary L_1 with L_2 and p^2 with p^3, we are back again in the cases (i), (ii), (iii) or (iv) of Remark 5.7, also not guaranteeing that the distance between those lines defines the width of C, but knowing that the angle between L_1 and $[p^2,p^3]$ (if (i), (ii) or (iv) hold) or L_1 and $[p^1,p^3]$ (if (iii) holds) is acute (see Figure 23).

(c) In the last step of the transformation of C we only move $c+r\mathbb{B}$ and L_1,L_2, keeping $r(C),D(C)$, and $R(C)$ constant. Independently of the tangencies (i)–(iv) of Remark 5.7, $c+r\mathbb{B}$ is translated until it becomes tangent with the pair of arcs with centers p^1,p^2 and radius $D(K)$, finishing the transformation of C into $\mathrm{BI}_{r,\gamma}$. Finally L_1 is rotated around p^1 (in case of (iii) of Remark 5.7) or around p^2 (in all other cases) keeping it tangent to $c+r\mathbb{B}$ and L_2 as well as keeping it parallel to L_1 and supporting C. A simple but crucial observation is the following: assuming that L_1 contains p^2, it was shown in (lb_3) of Subsection 4.3 that $c+r\mathbb{B}$ is the inball of $\mathrm{BP}_{r,\gamma}$, touching its boundary in the arcs with centers in p^1,p^2 of radius $D(K)$ and in L_1. Hence any translation of $c+r\mathbb{B}$ within the region spanned by the two arcs would lead to an intersection of L_1 with the interior of $c+r\mathbb{B}$. The former means that before the rotation of L_1, its angle with $[p^2,p^3]$ was not smaller than after. This observation implies that the breadth $b_s([p^2,p^3])$ with s orthogonal to the two lines is reduced by the rotation.

However, in Cases (ii) and (iii) of Remark 5.7 it obviously holds $b_s([p^2,p^3]) = d(L_1,L_2)$ and since $d(L_1,L_2)$ did not increase in any step of the transformation we obtain that $w(K) \geqslant d(L_1,L_2) \geqslant w(C)$.

Finally, consider the remaining Cases (i) and (iv): they describe the extremal situation when C shares its radii with a set from the edges $(\mathbb{BT},\mathbb{H})$ or $(\mathbb{BT},\mathbb{FR})$. In case of (i) L_1 and L_2 support $c+r\mathbb{B}$, which means $d(L_1,L_2) = 2r$ and therefore that $w(C) = d(L_1, L_2) \leqslant w(K)$. In case of (iv) we have $L_1 \supset [p^1, p^2]$ and $p^3 \in L_2$ parallel to L_1. Hence $w(C) \leqslant d(L_1, L_2) = w(\mathrm{I}_\gamma)$, within the given parameters for γ, and since $\mathrm{I}_\gamma \subset C$ it follows $w(C) = d(L_1, L_2)$. □

Proof of Theorem 3.2. As before we abbreviate $r(K) = r$ and the same for the other radii. In order to show the general validity of the inequality (lb_3), we split the proof into the following cases:

$$\text{(i)}\quad 8r \geqslant 3D, \gamma \geqslant \gamma_r, r \leqslant r(\mathbb{H}), \qquad \text{(ii)}\quad 8r < 3D$$
$$\text{(iii)}\quad \gamma < \gamma_r, r(\mathbb{BT}) \leqslant r \leqslant r(\mathbb{H}), \qquad \text{(iv)}\quad r > r(\mathbb{H}).$$

Recognize that in case of (i) there exists a bent pentagon $\mathrm{BP}_{r,\gamma}$, as we have shown with the help of Lemma 4.2 in (lb_3). Thus we are under the conditions of Lemma 5.8 in that case.

In the remaining cases, consider the generalized bent pentagon $\mathrm{BP}_{r,\gamma}$ as defined in the description of the facet (lb_3) (together with all the notation used there) and observe that the distance $d(L_1, L_2)$ may in any case be computed as the width in (6). The angle β may become $-\beta$ in Case (ii) (cf. Figure 24) or the angle μ may become $-\mu$ in Cases (iii) or (iv), whenever the angle between L_1 and $[p^2, p^3]$ is bigger than $\pi/2$. In both cases this change of sign does not affect the final value of the right hand side of the inequality (lb_3) to coincide with $d(L_1, L_2)$.

Hence it suffices to show $w \geqslant d(L_1, L_2)$. To do so, let us assume w. l. o. g. that $[p^1, p^2]$ is horizontal and below 0, that $p^1_1 \leqslant p^2_1$, and that $p^3_2 \geqslant 0$.

In case of (ii), Part (a) of Lemma 4.2 ensures that $[p^1, p^2]$ does not intersect $c + r\mathbb{B}$. Thus the slope of the lines L_i, $i = 1, 2$ is negative, and considering the line L containing $[p^1, p^2]$, the angle between L_1 and $[p^2, p^3]$ is smaller than the angle between L and $[p^2, p^3]$ (cf. Figure 24). Hence, denoting the line containing p^3 and parallel to L by L', we obtain $d(L_1, L_2) \leqslant d(L, L') = w(\mathrm{I}_\gamma) \leqslant w$.

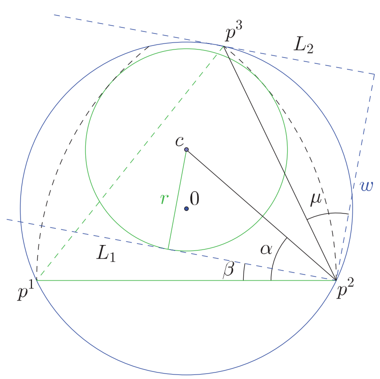

Figure 24: *If* $3D > 8r$, *the angle* β *in the computations in* (lb_3) (cf. *Figure* 15(a)) *becomes* $-\beta$, *but does not change the final equation for* $d(L_1, L_2)$.

Now, let us assume that (iii) is true, but not (ii). Then we know from Part (b) of Lemma 4.2, that the distance $d(L_1,L_2)$ decreases if γ decreases. Using $\gamma \leqslant \gamma' = \gamma_r$ we obtain that $d(L_1,L_2) \leqslant d(L_1',L_2') = w(\mathrm{BI}_{r,\gamma_r}) = 2r \leqslant w$.

Finally, for the treatment of (iv), one should first observe two easy facts: first, since $p^2 \in L_1$ and $p^3 \in L_2$ we have $d(L_1,L_2) \leqslant \|p^2 - p^3\|$ and second if $r = r(\mathbb{H}), \gamma = 2\arccos(D(\mathbb{H})/2)$, and $L_1^{\mathbb{H}}, L_2^{\mathbb{H}}$ are the corresponding support lines of $\mathbb{H}$, then $L_1^{\mathbb{H}}, L_2^{\mathbb{H}}$ are perpendicular to $[p^2,p^3]$ and thus $\|p^2 - p^3\| = w(\mathbb{H}) = 2r(\mathbb{H})$ (cf. the description of $\mathbb{H}$ in Subsection 4.1). From (iv) and inequality (ib_2) we obtain that $D(\mathbb{H}) = r(\mathbb{H}) + 1 \leqslant r + 1 \leqslant D$ and since $[p^2,p^3]$ is the shorter edge of I_γ we have $\|p^2 - p^3\| = D/R\sqrt{4R^2 - D^2}$ which is a decreasing function in D. Hence $\|p^2 - p^3\|$ is maximized, when $\gamma = \gamma_r$, i. e. when $\|p^2 - p^3\| = w(\mathbb{H})$. Thus using inequality (lb_1) we obtain that

$$d(L_1,L_2) \leqslant \|p^2 - p^3\| \leqslant w(\mathbb{H}) = 2r(\mathbb{H}) \leqslant 2r \leqslant w,$$

which completes the proof. □

6. Final remarks

For finishing the paper, let us give two final remarks:

First, for some practical purposes it could be of some value to be able to replace the sometimes quite unhandy non-linear inequalities by linear ones. Thus knowing the full extend of the diagram now, it would be worthwhile to develope a complete system of linear inequalities supporting the diagram. Since the convex hull of the vertices does not contain the full diagram (the supporting plane of $\mathbb{L}, \mathbb{I}_{\pi/3}$, and $\mathbb{I}_{\pi/2}$ separates $\mathrm{SB}_\gamma^{\circledcirc}$ from major parts of the diagram) and since all edges and facets are smooth, this system cannot be finite.

Second, especially considering the application of Blaschke-Santaló diagrams given in [7, 8, 17], consider the following problem: suppose two convex sets K and K' are mapped to the same point in the diagram, how "different" may K and K' be? For this neither the usual Hausdorff nor the Banach-Mazur distance can be taken. For the Hausdorff distance any K and some of its rotations may be quite far from each other, while the Banach-Mazur distance would mark (e. g.) all simplices equal. A good choice for this task could be taking the Hausdorff distance within the class of similarities of the two sets (cf. [11]).

Acknowledgements. We would like to thank Viviana Ghiglione and Evgeny Zavalnyuk for giving crucial hints, as well as Peter Gritzmann, Maria Hernández Cifre, and Salvador Segura Gomis for always supporting us.

REFERENCES

[1] W. BLASCHKE, *Eine Frage Über Konvexe Körper*, Jahresber. Deutsch. Math. Ver., **25** (1916), 121–125.

[2] T. BONNESEN, W. FENCHEL, *Theorie der konvexen Körper*, Springer, Berlin, 1934, 1974, english translation: *Theory of convex bodies*, edited by L. Boron, C. Christenson and B. Smith, BCS Associates, Moscow, ID, 1987.

[3] K. BÖRÖCZKY JR., M. A. HERNÁNDEZ CIFRE AND G. SALINAS, *Optimizing area and perimeter of convex sets for fixed circumradius and inradius*, Monatsh. Math., **138** (2003), 95–110.
[4] R. BRANDENBERG, *Radii of convex bodies*, Ph. D. thesis, Zentrum Mathematik, Technische Universität München, 2002.
[5] R. BRANDENBERG, S. KÖNIG, *No dimension-independent core-sets for containment under homothetics*, Discrete Comput. Geom., **49** (1) (2013), 3–21.
[6] R. BRANDENBERG, S. KÖNIG, *Sharpening geometric inequalities using computable symmetry measures*, Mathematika, **61** (3) (2015), 559–580.
[7] J. DEBAYLE, J. C. PINOLI AND B. PRESLES, *Shape recognition from shadows of 3-D convex geometrical objects*, 19th IEEE International Conference on Image Processing (ICIP), 2012, 509–512.
[8] J. DEBAYLE, S. RIVOLLIER AND J. C. PINOLI, *Adaptive Shape Diagrams for Multiscale Morphometrical Image Analysis*, J. Math. Imaging Vis. 2013.
[9] B. V. DEKSTER, *An extension of Jung's theorem*, Israel J. Math., **50** (3) (1985), 169–180.
[10] P. GRITZMANN, V. KLEE, *Inner and outer j-radii of convex bodies in finite-dimensional normed spaces*, Discrete Comput. Geom., **7** (1992), 255–280.
[11] B. GONZÁLEZ MERINO, N. JONARD-PÉREZ, *A pseudometric invariant under similarities in the hyperspace of non-degenerated compact convex sets of R^n*, Topology Appl., **196** (2015), 125–143.
[12] M. A. HERNÁNDEZ CIFRE, *Is there a planar convex set with given width, diameter and inradius?*, Amer. Math. Monthly, **107** (2000), 893–900.
[13] M. A. HERNÁNDEZ CIFRE, *Optimizing the perimeter and the area of convex sets with fixed diameter and circumradius*, Arch. Math., **79** (2002), 147–157.
[14] M. A. HERNÁNDEZ CIFRE, E. SAORÍN, *On the roots of the Steiner polynomial of a 3-dimensional convex body*, Adv. Geom., **7** (2007), 275–294.
[15] M. A. HERNÁNDEZ CIFRE, S. SEGURA GOMIS, *The missing boundaries of the Santaló diagrams for the cases (d,w,R) and (w,R,r)*, Discrete Comp. Geom., **23** (2000), 381–388.
[16] H. JUNG, *Über die kleinste Kugel, die eine räumliche Figur einschließt*, J. Reine Angew. Math., **123** (1901), 241–257.
[17] B. PRESLES, *Caractérisation géométrique et morphométrique 3D para analyse d'images 2D de distributions dynamiques de particules convexes anisotropes*, Ph. D. Thesis, 2011.
[18] J. R. SANGWINE-YAGER, *The missing boundary of the Blaschke diagram*, Amer. Math. Monthly, **96** (1989), 233–237.
[19] L. SANTALÓ, *Sobre los sistemas completos de desigualdades entre tres elementos de una figura convexa planas*, Math. Notae, **17** (1961), 82–104.
[20] R. SCHNEIDER, *Convex Bodies: The Brunn-Minkowski Theory*, Cambridge University Press, Cambridge, 1993.
[21] P. R. SCOTT, *Sets of constant width and inequalities*, Quart. J. Math. Oxford Ser., **32** (1981), 345–348.
[22] P. STEINHAGEN, *Über die größte Kugel in einer konvexen Punktmenge*, Abh. Hamb. Sem. Hamburg, **1** (1921), 15–26.
[23] L. TING, J. B. KELLER, *Extremal convex planar sets*, Discrete Comput. Geom., **33** (2005), no. 3, 369–393.

(Received June 20, 2015)

René Brandenberg
Zentrum Mathematik
Technische Universität München
Boltzmannstr. 3, 85747 Garching bei München, Germany
e-mail: brandenb@ma.tum.de

Bernardo González Merino
Zentrum Mathematik
Technische Universität München
Boltzmannstr. 3, 85747 Garching bei München, Germany
e-mail: bg.merino@tum.de